

UNCERTAINTY ASSESSMENT IN PROJECTION OF THE EXTREME RIVER
FLOWS: THE CASE OF OMERLI CATCHMENT, ISTANBUL

A THESIS SUBMITTED TO
THE GRADUATE SCHOOL OF NATURAL AND APPLIED SCIENCES
OF
MIDDLE EAST TECHNICAL UNIVERSITY

BY

BATUHAN EREN ENGIN

IN PARTIAL FULFILLMENT OF THE REQUIREMENTS
FOR
THE DEGREE OF MASTER OF SCIENCE
IN
EARTH SYSTEM SCIENCE

FEBRUARY 2015

Approval of the thesis:

**UNCERTAINTY ASSESSMENT IN PROJECTION OF THE EXTREME
RIVER FLOWS: THE CASE OF OMERLI CATCHMENT, ISTANBUL**

submitted by **BATUHAN EREN ENGIN** in partial fulfillment of the requirements
for the degree of **Master of Science in Earth System Science, Middle East
Technical University** by,

Prof. Dr. Gülbin DURAL ÜNVER _____
Dean, Graduate School of **Natural and Applied Sciences**

Prof. Dr. Ayşen YILMAZ _____
Head of Department, **Earth System Science**

Assoc. Prof. Dr. İsmail YÜCEL _____
Supervisor, **Civil Engineering Dept. / Earth System Science**

Prof. Dr. Ayşen YILMAZ _____
Co-Supervisor, **Institute of Marine Sciences / Earth System Science**

Examining Committee Members:

Prof. Dr. Ayşen YILMAZ _____
Institute of Marine Sciences / Earth System Science Dept., METU

Assoc. Prof. Dr. İsmail YÜCEL _____
Civil Engineering Dept. / Earth System Science Dept., METU

Prof. Dr. Ramazan SARI _____
Business Administration Dept. / Earth System Science Dept., METU

Assistant Prof. Koray YILMAZ _____
Geological Engineering Dept. / Earth System Science Dept., METU

Assistant Prof. Tuğrul YILMAZ _____
Civil Engineering Dept, METU

Date: 06.02.2015

I hereby declare that all information in this document has been obtained and presented in accordance with academic rules and ethical conduct. I also declare that, as required by these rules and conduct, I have fully cited and referenced all material and results that are not original to this work.

Name, Last Name: Batuhan Eren ENGIN

Signature:

ABSTRACT

UNCERTAINTY ASSESSMENT IN PROJECTION OF THE EXTREME RIVER FLOWS, THE CASE OF OMERLI CATCHMENT, ISTANBUL

Engin, Batuhan Eren

M.S., Department of Earth System Science

Supervisor: Assoc. Prof. Dr. İsmail Yücel

Co-Supervisor: Prof. Dr. Ayşen Yılmaz

February 2015, 68 Pages

The average temperature at the surface of the Earth has been increasing over the past century due to the increased greenhouse gases concentrations in atmosphere through anthropogenic activities. Rising temperature leads to an increase in evaporation and thus intensifies the components of water cycle which results in extreme flows in different parts of the world through changes in globally averaged precipitation. Projection of extreme flows is very important in this aspect, yet obscurity about many factors that would influence future climate causes great uncertainty in climate variable prediction. Therefore, in this research, it is intended to quantify relative contribution to the uncertainty in extreme flow (high and low) projection change for the future period by two factors, the parameterization of a hydrological model and temperature and precipitation inputs from fifteen different Regional Climate Models (RCM), for Omerli Catchment area, in Istanbul. The uncertainty due to the precipitation and temperature inputs is investigated by using 15 different RCMs and also by applying two different statistical downscaling (SD) methods to the RCMs outputs for the

reference (1961-1990) and future (2071-2099) period, “Bias Correction in Mean” and “Change Factor”. The uncertainty due to the hydrological parameterization (HP) of the hydrological model is assessed by using 25 different parameter sets generated by Monte-Carlo simulation technique using 5 different Nash functions as the objective function during the calibration of the hydrological model, which are NSE_Normal, NSE_BL, NSE_p3, NSE_Viney and NSE_Weighted. Observed daily precipitation and temperature records are provided by Turkish State Meteorological Service for the period 1961-2004, while daily discharges are obtained from State Hydraulic Works for the period 1978-2004. In converting the precipitation and temperature from RCMs into discharges, the HBV Hydrological model is used, which is calibrated to the period 1978-1985 and validated for the period 1986-2004. Main finding is that the relative contribution to the uncertainty by the temperature and precipitation inputs from different regional climate models is greater than the uncertainty caused by hydrological model parameterization in prediction of extreme high flow events in each data type: Original RCM, BC and CF methods. BC and CF increase the total mean variance in the changes in extreme high flow and low events from reference to future period. It is found that the observed dominant high flow events mostly occur during autumn/winter season for the reference period. Simulations using Original RCM, BC and CF data overestimate the seasonality index for the reference period. For the future period, simulations by parameter files using BC and CF data projected that the seasonality in high flow events will be stronger than their reference period, which means that in the future the Omerli catchment would likely to observe more dominant high flow events in autumn/winter.

Keywords: Climate Change, Extreme flow prediction, Uncertainty assessment, Statistical Downscaling, Seasonality, Omerli Basin

ÖZ

EKSTREM AKIM TAHMİNLERİNDEKİ BELİRSİZLİKLERİN DEĞERLENDİRİLMESİ: ÖMERLİ HAVZASI, İSTANBUL

Engin, Batuhan Eren

Yüksek Lisans, Yer Sistem Bilimleri Bölümü

Tez Yöneticisi: Doç. Dr. İsmail Yücel

Ortak Tez Yöneticisi: Prof. Dr. Ayşen Yılmaz

Şubat 2015, 68 Sayfa

Dünya yüzeyinin ortalama sıcaklığı son yüzyılda antropojenik etkilerden dolayı atmosfere salınan Sera Gazları sebebiyle giderek artmaktadır. Yükselen sıcaklıklardan dolayı artan buharlaşma, su döngüsündeki bileşenleri etkileyerek dünyanın farklı havzalarında kuraklığa veya sel felaketlerine sebep olmaktadır. Bu bağlamda, ekstrem akımların tahmin edilmesi önem arz etmektedir ancak, sera gazlarının gelecek dönemdeki salınımının kestirilememesi, ayrıca gelecekteki iklimi etkileyebilecek faktörlerdeki bilinmezlik, iklim tahminlerinde önemli bir belirsizliğe sebep olmaktadır. Bu sebeple bu çalışmada Ömerli havzası için, hidrolojik parametrelendirme ve farklı iklim tahmin modellerinin ekstrem akımların tahmin edilmesinde ortaya çıkan belirsizlikteki göreceli payın araştırılması amaçlanmıştır. 1978-2004 yılları günlük gözlem yağış ve sıcaklık verileri Devlet Meteoroloji Müdürlüğü, Ömerli havzasına ait bir istasyondan alınan akım değerleri Devlet Su İşleri tarafından sağlanmıştır. HBV hidrolojik modeli, 1978-1985 yıllarına, gözlem akım değerleri kullanılarak kalibre edilmiş ve bunun sonucunda Monte-Carlo simülasyonu

aracılığıyla 5 farklı NSE fonksiyonuna göre kalibre edilmiş ve 25'er parametre dosyası elde edilmiştir, ve model 1986-2004 yılları için kontrol edilmiştir. Bu çalışmada, 15 farklı Bölgesel İklim Modelinin (RCM) 25 km mekansal çözünürlüğe sahip verileri kullanılmıştır. Ayrıca, RCMler'in kontrol ve gelecek dönem sıcaklık ve yağış verilerine "Bias Correction" (BC) ve "Change Factor" (CF) istatistiksel ölçek küçültme metodu uygulanmıştır. Çalışma sonunda bulunan temel bulgu, her üç veri tipi için de, farklı iklim tahmin modellerinin, ekstrem akımları tahmin etmedeki toplam belirsizlikteki payının, hidrolojik parametrelendirmeye göre daha fazla olduğudur. Ayrıca, BC ve CF metodlarının tahmin edilen ekstrem akımlar içindeki toplam ortalama varyansı arttırdığı saptanmıştır. BC metodunda hidrolojik model parametrelendirmenin belirsizliğe katkısı RCMler'e göre daha az olmuştur. 1961-1990 yılları için gözlemlenmiş ekstrem pik akımların, sonbahar/kış mevsimlerinde daha güçlü olduğu saptanmıştır. RCMler'in çıktılarını kullanılarak yapılan hidrolojik simülasyonlar, gözlem periyodu için gerçekleşenden daha güçlü bir mevsimsellik tahmin etmiştir. BC ve CF verileri kullanılarak yapılan simülasyonlar gelecek dönem için, gözlem periyoduna oranla mevsimselliğin biraz daha güçleneceğini öngörmüştür. İstatistiksel ölçek küçültülen verileriyle yapılan bu simülasyonlar Ömerli Havzası'nın gelecek dönem sonbahar/kış aylarında daha baskın (kuvvetli) pik akımlar yaşanacağını tahmin ettiğini göstermektedir.

Anahtar Kelimeler: İklim Değişikliği, Ekstrem akım tahmini, İstatistiksel Ölçek Küçültme, Belirsizlik değerlendirme, Mevsimsellik, Ömerli Havzası

To nature

ACKNOWLEDGEMENT

I would like to thank to my supervisor, Assoc. Prof. Ismail YUCEL, for his continuous insistence on me to finish this thesis and his patience and invaluable support. I would have never been able to complete the study without his support.

I would like to thank to my co-advisor Prof. Ayşen YILMAZ for her precious contribution to this study who played an important role in all of my three approvals to the Earth System Science program, I would not have had this life changing opportunity without her. Also, I would like to thanks to the members of jury for their consructive criticism.

ESS family deserves a sincere gratitude for their friendship and support. I would like to express my sincere gratitude to the ones who created MATLAB. Without it, handling with enormous data would be terribly problematic.

This study was supported by TÜBİTAK with project number 110Y036 and COST Action ES0901“European Procedures for Flood Frequency Estimation (FloodFreq)” (<http://www.cost-floodfreq.eu/>).

TABLE OF CONTENTS

ABSTRACT	v
ÖZ.....	vii
ACKNOWLEDGEMENT	x
TABLE OF CONTENTS	xi
LIST OF TABLES.....	xiii
LIST OF FIGURES	xiv
LIST OF ABBREVIATIONS	xvi
CHAPTERS	
1. INTRODUCTION	1
1.1. Research Background and Motivation.....	1
1.2. Literature Review.....	2
1.2.1. Climate Change Impacts	2
1.2.2. Uncertainty in Climate Models	4
1.2.3. Uncertainty in Hydrological Model Outputs.....	6
1.2.4. Uncertainty Measure Techniques.....	7
1.2.5. Studies on Climate Change Impact Assessment in Turkey.....	8
1.2.6. Review on Downscaling.....	10
1.2.7. Change factor and Bias Correction in Mean Methods	12
1.3. Problem Statement	14
2. STUDY AREA, DATA AND MODELS	15
2.1. Study Area and Data Set	15
2.2. Observed Data Set.....	16
2.3. Climate Models Data Sets.....	17
2.4. Hydrological Model	18
3. METHODOLOGY	21
3.1. HBV Hydrological Model Calibration.....	21

3.1.1. Objective Functions of Calibration	22
3.1.2 Calibration Procedure	23
3.2. Multi Decision Making Method- TOPSIS.....	25
3.3. Statistical Downscaling Methods	26
3.3.1. Change Factor Method.....	26
3.3.2. Bias Correction in Mean Method.....	27
3.4. Extreme Value Series	28
3.5. Uncertainty Assessment	29
3.6. Seasonality.....	31
3.7. Organizing Essential Data	31
4. PRECIPITATION ANALYSIS	33
4.1. Evaluation of RCMs precipitation.....	33
5. RESULTS and DISCUSSION	39
5.3. Uncertainty Analysis for Runoffs from Reference To Future Periods ...	45
5.3.1. Uncertainty in High Flow Prediction.....	45
5.3.2. Uncertainty in Low Flow Prediction.....	48
5.4. Seasonality.....	50
5.4.1. High flow Analysis	50
6. SUMMARY, CONCLUSIONS and RECOMMENDATIONS.....	57
6.1. Summary.....	57
6.2. Conclusions	58
6.3. Future Work Recommendations	61
REFERENCES.....	63

LIST OF TABLES

TABLES

Table 2.1. List of RCMs used in the study	18
Table 4.1. RCM's performance indicators for the reference period 1961 -1990	35
Table 4.2. The Weights assigned to criteria	36
Table 4.3. Sorted RCMs based on TOPSIS Grades	36
Table 5.1 Performance indicators for the parameter sets for validation period 1986-2004 (Green and red backcolor indicate the best and worst values in each criterion)	41
Table 5.2. Averaged performance indicators of 25 parameter files for each NSE function	42
Table 5.3. Sorted parameter files with respect to the TOPSIS Grades.....	43
Table 5.4. Calculated mean variances among RCMs (Var_RCM) and hydrological model parameters (Var_Hydro) for high flows obtained through downscaled and no downscaled precipitation and temperature.....	46
Table 5.5. Calculated mean variances among RCMs (Var_RCM) and hydrological model parameters (Var_Hydro) for low flows obtained through downscaled and no downscaled precipitation and temperature.....	48

LIST OF FIGURES

FIGURES

Figure 1.1. IPCC Climate Scenarios Family	6
Figure 1.2. Uncertainty components (Dobler et al., 2012).....	8
Figure 2.1. Omerli Catchment (Andrew Byfield and Neriman Özhatay, 2009)	15
Figure 2.2. Omerli Catchment (I. Yucel, FLOODREQ Project, 2010)	17
Figure 4.1 - RMSE, NSE, Correlation Coefficient R and Bias measures of 15 RCMs in deriving daily precipitation.....	33
Figure 4.2. Averaged daily precipitation of RCMs for the period 1961-1999..	37
Figure 5.1. Boxplot of simulated and observed discharges for the period 1986- 2004.....	40
Figure 5.2. Boxplot of simulated and observed high flow discharges for the period 1986-2004	44
Figure 5.3. Boxplot of simulated and observed low flow for the period 1986- 2004.....	45
Figure 5.4. The fractions of total variance as a measure for uncertainty in the change in mean high flow events due to HP and RCMs	47
Figure 5.5. The fractions of total variance as a measure for uncertainty in the change in mean low events due to HP and RCMs	49
Figure 5.6. Boxplot showing seasonality index for both period for each data type, (SD_obs indicates the observed seasonality)	51
Figure 5.7 Uncertainty in seasonality due to hydrological model parameterization (a) and climate models	53
Figure 5.8 Uncertainty in seasonality due to hydrological model parameterization (a) and climate models	54
Figure 5.9 Uncertainty in seasonality due to hydrological model parameterization (a) and climate models	55
Figure 5.10 Uncertainty in seasonality due to hydrological model parameterization (a) and climate models (b) (Each box plot contains all	

simulations by every parameter files from each NSE function) (Purple line indicates the observed seasonality from the reference period)..... 56

LIST OF ABBREVIATIONS

PPM	Parts per million
DDS	Dynamically Dimensioned Search method
NSE	NSE-Sutcliffe-Efficiency
RMSE	Root Mean Square Error
GCM	Global Circulation Model
RCM	Regional Climate Models
GDSHW	General Directorate of State Hydraulic Works
SD	Statistical Downscaling
BC	Bias Correction in Mean
CF	Change Factor

CHAPTER 1

INTRODUCTION

1.1. Research Background and Motivation

The average temperature of the Earth's surface has been showing an accelerated warming trend over the late twentieth-century due to the both natural and human-induced forcing, but a recently scientific research showed that, by providing a link between greenhouse gases and temperature, it is mainly due to rapidly increasing greenhouse gas concentrations through anthropogenic activities such as burning fossil fuels, deforestation and desertification, use of chemical fertilizers, depletion of ozone layer due to the industrialization, land use etc. (Jay Gulledge, July 2012; Meehl et al., 2004).

Since the greenhouse gas molecules, clouds and water vapor in the air absorb and re-radiate most of the infrared radiation emitted by the Earth's surface in all directions, the temperature of the Earth's surface rises up, which is called the greenhouse effect in general. Increasing proportion of greenhouse gases such as CO₂ intensifies the greenhouse effect, which causes Earth to get warmer, which leads to an increase in evaporation. Furthermore, growing concentration of water vapor in the air further amplifies the greenhouse effect, as the water vapor is the most effective greenhouse gas, and thus this process forms a positive feedback loop which would eventually cause Earth's atmosphere and surface gets warmer incrementally (Le Treut, 2007).

According to the report published in 2013 on climate change by "Intergovernmental Panel on Climate Change" (IPCC), the concentration of carbon dioxide (CO₂) has increased by more than 40% since 1750 and reached its peak at 390.5 parts per million (ppm) recently (Observatory, 2015), and

atmospheric nitrous oxide (N₂O) has risen by 20% since 1750. The globally averaged land and ocean surface temperature has increased 0.85 °C (90% confidence interval: 0.65 - 1.06°C) over the period 1880-2012 (Hartmann, 2013). According to the IPCC's "Special Report on Emission Scenarios" published in 2007, the atmospheric concentration of CO₂ is projected to reach 600 ppm by 2099 and the global averaged surface temperature to rise likely by a range of 1.1-2.9 °C by 2099 relative to 1980-1990 even under B1 low emission scenario where the world is more integrated and more ecologically friendly.

1.2. Literature Review

1.2.1. Climate Change Impacts

The impacts of climate change on nature have begun to wreak its havoc across the globe. Rising sea levels will threaten to wash away Pacific island states, coastal cities or agricultural areas around the coastal place and severely affect the local people inhabited the area if the projection by IPCC comes true stating that the sea level could rise by as much as 5 mm per year over the next decade due to ice sheets and glaciers melting plus due to expansion of oceans because of warming.

Hurricanes and tropical storm are another socio-economic natural catastrophe that could be influenced by climate change. As the hurricanes and tropical storms form over the ocean, suggesting that higher sea temperature could strengthen the impact of hurricanes, scientists anticipate the intensity and frequency of hurricanes and tropical storm to rise, although some say that there is no clear data to suggest that there is an "increased trend in the intensity and frequency of hurricanes", as stated in (2010).

Agricultural sector is also affected by the climate change. With higher temperature, weed and pest are more likely to grow while the desirable crops yield is likely to decline. Also, shifting precipitation patterns resulting in

unexpected flood and drought conditions could lead to undesirable crop loss. Since not only the available amount of usable water for agricultural practices diminish but also the water quality, the crop yield will also decrease. Therefore the prices in food chain can be expected to rise, resulting in socio economic impacts and posing hazards to people belonging especially to low and mid class (Fischer et al., 2005).

One of the most vital impacts of climate change is its impacts on water resources, as this thesis investigates a small but important part of them. It is suggested that the rising temperature will cause the precipitation type to shift from snowfall to rainfall (Feng et al., 2007). Rapid snow melting and the shift from snowfall to rainfall could all together prevent the water infiltrate to the ground and thus join surface runoff which could pose problem for the elevated areas where agricultural and urban water necessities are regulated through the snow load over a year (Environment, July 2011).

Soil moisture changes, decline in water chemical, biological and thermal quality, droughts or floods, reduced ground water recharge, water scarcity, dam failure because of floods are also some of the potential impacts of climate change on water according to M. El-Fadel et al. study (Bou-Zeid et al., 2002).

As the world already began to witness today, observed rising globally averaged temperature tends to increase the uncertainty and instability in precipitation patterns and trends, thus dramatically altering the frequency and magnitude of extreme rainfalls, resulting in drought and flood conditions in different parts of the world even in the regions in which the average annual precipitation is predicted to decrease (Frei et al., 2006). It is no doubt that these extreme conditions exert great distress on societies and needs to be taken care of. Therefore, in this research it is intended to quantify relative contribution to the uncertainty in projected extreme flow (high and low) change for the future period by two factors, hydrological parameterization and climate projection models, for Omerli Catchment area, in Istanbul.

1.2.2. Uncertainty in Climate Models

According to Smith et al. (2002), it has been achieved that the past 150 years of earth climate history has been modeled “within the observed uncertainty of the observations”. They estimated the uncertainty in model outputs mainly caused by the variability of climate system itself, by comparing three separate runs of a climate model fed with same “Greenhouse gases and sulfate aerosols level” but initiated with different conditions. By doing these analyses, the conclusion they have come up with is that the uncertainty in observations is high when compared to the variability in modeled temperature trends. However, they also emphasized that since the model used only a single climate forcing as input, the uncertainty incurred by different climate forcings in model outputs were neglected.

The uncertainty in climate models, or in future climate to speak, could stem from several culprits. According to the M. Petrakis (2014), about half of the future uncertainty in temperature and therefore in climate is due to the uncertainty in future CO₂ and GHG gases emission levels, which will determine the condition of future climate. GHG gases emission are driven by forces such as demographic, socio-economic and technological development throughout the world, policies that countries implement, etc. Scientists from IPCC in 2007 have developed emissions scenarios (Figure 1.1 - IPCC’s Climate Scenarios Family) to cover the probable range of emission levels which give us insight about how the future might evolve and how those driving forces might affect future emission. Of course, as they are not assigned any probability of occurrence, it cannot be said that one emission scenario is more likely than another (Kalra, 2014). Any of predetermined climate scenarios depicting the future climate in different conditions cannot predict it precisely. Therefore, it cannot be said that running a climate model under all predetermined climate scenarios disregards the uncertainty of forecasting future climate, but in fact it helps to reduce it. Therefore, it is best to use the outputs of several climate models under several climate scenarios to reduce the uncertainty belonging to future and to capture the probabilistic range of climate change, yet this solution surely increases the computational effort.

Another source of uncertainty could be emerged from the fact that the models do not/cannot include all of the physical, chemical processes, or feedback mechanisms that can affect the climate. Some of those processes need to be omitted in climate models, not just because they are unexplained yet, but also due to the insufficient computational power (OCAR, 2010).

It can be given two examples to the feedback mechanisms that play a vital role in uncertainty in climate models; cloud feedback and ice/snow feedback. These feedback mechanisms are extremely complex to understand and formulize. As climate models represent these feedbacks differently parameterized to each other, uncertainty between models comes to light (OCAR, 2010). There could also be unexplained climate phenomenon influencing the climate throughout the world by teleconnections which the models may not predict precisely, so the uncertainty in model prediction occurs. Until recently the climate models have not include them, but they have started to include most of the processes inherent in climate systems as the climate models have been improved vastly in the last decades.

Chaotic behavior of the climate system is the main reason of its natural variability. GCMs might be able to reproduce average conditions for a short period of time, however, it is very hard for GCMs to capture and analyze the climate variability. Although the prediction models are developed by observing the past climate and modeling according to the probable future conditions, it does not necessarily mean that the models can reproduce the full range of variability that can be in future climate. Therefore, without understanding the very complex nature of climate patterns, it cannot be said that model prediction of future climate can avoid the uncertainty completely (Reichler T, 2008).

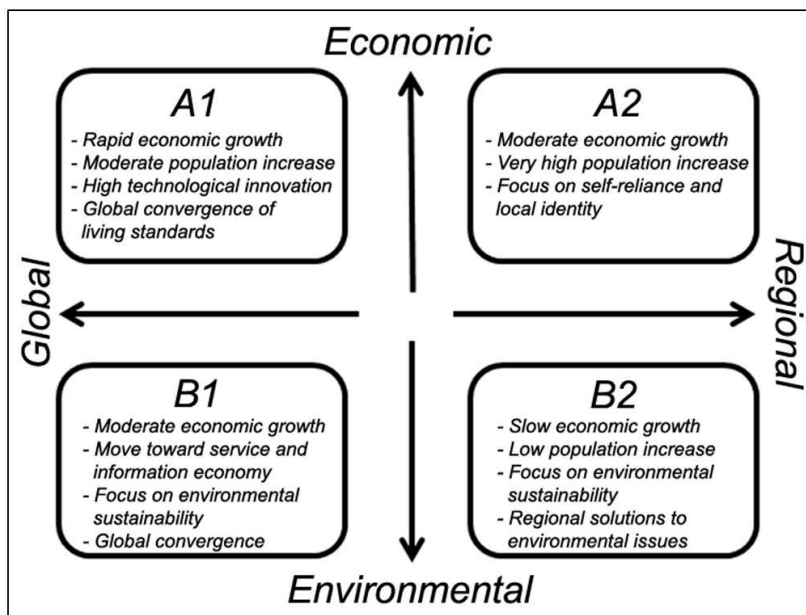


Figure 1.1. IPCC Climate Scenarios Family

Uncertainty might not only arise from hydrological models, but also from the data. Recording observation for a short time period may not be sufficient to represent natural variability; in addition to that, measurement of data may not be so accurate. Therefore, sampling frequency and methods need to be paid attention for the uncertainty (Prudhomme et al., 2003).

1.2.3. Uncertainty in Hydrological Model Outputs

As it is explained in the Chapter 1, assessing uncertainty in projections of future climate variables has been an important subject of study in recent years. Hydrological model parameterization is considered as an important source of uncertainty in future rainfall-runoff prediction and drawing an increasing attention among the scientists. According to Lindenschmidt (2007), uncertainty in hydrological model outputs consists of three components: model structure, input data and parameterization. In this thesis, only the uncertainty in future runoff prediction caused by parameterization is concerned.

1.2.4. Uncertainty Measure Techniques

“Generalized Likelihood Uncertainty Estimation” (GLUE) method introduced by Beven et al. (1992) has been widely used in previous uncertainty assessment studies for “its simplicity and applicability to nonlinear systems” as stated in Stedinger et al. (2008). In GLUE method, Monte Carlo simulation is used and many parameter sets are produced. With each parameter set, model in question is run and the outputs are generated for the calibration period. And the goodness-of-fit, also called likelihood measure by Beven et al.(1992) is applied to assess the performance of each parameter set. Only parameter sets whose goodness-of-fit values are above a certain threshold are chosen and assigned a likelihood weight that sum to 1. These ranked parameter set are used to form a cumulative distribution for the variables on target afterwards. Finally, uncertainty intervals are determined by selecting quartiles from the cumulative distributions.

Z.Y. Shen et al. (2012) used a combination of GLUE and “Soil and Water Assessment Tool” (SWAT) method to assess the parameter uncertainty of discharge prediction. They stated that there are several techniques for calibration and uncertainty analysis used in previous studies, such as the “first-order error analysis” (FOEA), Monte Carlo method and GLUE. They also included some weak points for the methods except for GLUE. As cited by Z.Y. Shen et al. (2012), Melching et al. (1996) stated that FOEA gives poor result in representing complex environment, whereas Gong et al. (2011) stating that Monte Carlo requires tremendous computational time. They reported that the uncertainty calculated by GLUE method will account for all sources of parameter uncertainty, such as “input uncertainty, structural uncertainty, parameter uncertainty and response uncertainty”.

Dobler et al. (2012), worked on the quantification of uncertainties caused by GCMs, RCMs, Bias correction of RCMs and hydrological model parameterization, using three GCMs (ECHAM5, HadCM3, BCM), three RCMs (RCA, REMO, RACMO), three BC methods (Delta change, Local scaling and Quantile-Quantile mapping) and sets of different parameter range.

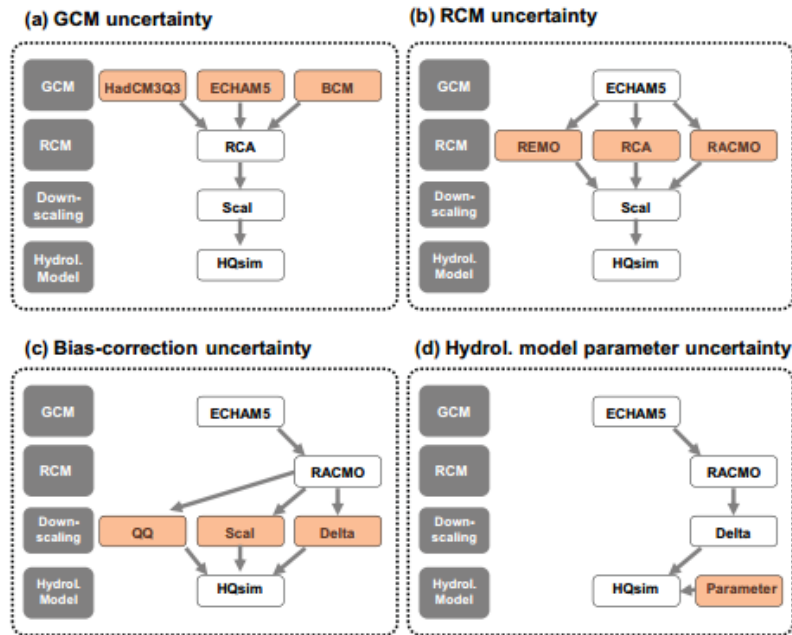


Figure 1.2. Uncertainty components (Dobler et al., 2012)

They assessed the influence of each source of uncertainty by varying the modelling component under focus one by one, while holding others constant, as it can be seen in Figure 1.2. To measure the contribution of the different sources to the overall uncertainty, they used the spread (percentage points) between different simulations, while it is also reported that they could use an analysis of variance (ANOVA) as an alternative. They concluded that the hydrological model parameter uncertainty which is evaluated by Monte Carlo simulation method is the least contributor to the overall uncertainty, while GCM and RCM accounts most for the overall uncertainty. They found that BC is the one having greatest influence on projections of extreme discharge.

1.2.5. Studies on Climate Change Impact Assessment in Turkey

Recently, the number of studies on climate change impact assessment for the hydrological basins of Turkey is growing, since it is realized that climate change will have severe impact on the climate and hydrological compounds of basins of Turkey. The Ministry of Environment and Urbanization published five national

declaration on climate change ever since Turkey acceded to the agreement, United Nations Framework Convention on Climate Change, in 2004. In the fifth report published in 2009, it is given that the most of the province of Turkey experienced statistically significant increase in temperature and decrease in precipitation amount throughout the period 1950-2010. It is mentioned that the Marmara region, where industrialization and urbanization mostly take place, also experienced the same change, yet more intensely. Bozkurt et al. (2012) downscaled several GCMs under different climate scenario for Turkey and projected that the surface temperature will increase for the period 2011-2040, but more warming will be observed for the period 2040-2070. They also projected that the surface runoff will increase for almost all province of Turkey including Omerli basins for both winter and spring season for the first 30 year period. Omerli catchment area will experience a slight increase in surface runoff for both winter and spring for the years 2011-2099 (Bozkurt et al., 2012). There are several studies on the influence of climate change on water resources in Turkey, reported in “5th Declaration on Climate Change, Turkey” (2013). A national project called “Change in Mediterranean Hydrology due to Climate: to reduce uncertainty using integrated monitoring and modeling and to quantify the risk” was implemented in Kocaeli basin in 2010 which focused on reducing the uncertainty in climate change impact assessment. A study on developing climate scenarios and impact assessment for Konya Basin and East Mediterranean Basin was implemented in 2010. Main objectives of basin scale hydrological modeling in this project were to analyze surface and groundwater sources for the current climate and the effect of climate change on water sources for future period. A study on the climate change impacts in the Euphrates – Tigris Basin was carried out by Bozkurt et al. (2013) which claimed that the basin will experience significant decreases in the annual surface runoff. Yucel et al. (2015) also showed very significant regional warming in eastern Anatolia that causes important temporal shifts in snow melt runoffs of Tiger, Euphrates, Aras, and Coruh rivers towards earlier times.

However, there are not any studies published on the assessment of uncertainty in projected changes in future surface runoff for the hydrological basins of Turkey, including Omerli basin. Therefore, this study is intended to provide a methodology that will set an example for other important hydrological basins of Turkey to be explored in terms of uncertainty in the projected changes in extreme discharge values.

1.2.6. Review on Downscaling

GCMs are the numerical models with coarse spatial resolution (around 150-200 km) used to model the present climate and to predict the future climate by representing physical processes in the atmosphere, ocean, cryosphere and land surface. Because of having relatively coarse spatial resolution, GCMs are not often sufficient to represent the variability in climate variables especially for the regions of complex topography, coastal or island locations and heterogeneous land cover etc., thus their results cannot be directly used in hydrological models for climate change impact studies at local scale. Therefore, it is needed to statistically downscale the temperature and precipitation obtained from GCMs/RCMs in order to have finer grid scale, which could result in more reliable impact assessment at local scale.

GCM outputs can be downscaled in two methods, dynamical (DD) and statistical downscaling. In dynamical downscaling, a mathematical model called Regional Circulation Model (RCM) of which boundary conditions are determined by one of the GCM outputs is used, thus RCMs can be said to represent a catchment characteristics better than GCMs (except for certain cases) as they have much smaller grid scales, typically 10-50 km. However, dynamical downscaling is hard to apply not only because RCMs require an additional large computational capacity but also the necessity of RCM predictions to be bias corrected before their direct-use, since they are driven by GCM predictions which are already biased (Maraun et al., 2010). RCMs spatial resolution may still be not adequate for the climate change impact assessment.

It must be noted that since dynamical downscaling is computational intensive, RCMs are run for time slices, e.g. normally 30 years for simulation and control period.

Statistical downscaling is used by establishing a relationship between large scale variables obtained from GCMs and local scale variables. Statistical downscaling methods are easy to apply due to requiring less computational effort. Another advantage of using statistical downscaling method is that once the relationship is established, it can be applied to output from different GCMs\RCMs. However, statistical downscaling methods can be disadvantageous to use in certain case where the stationary relationship between large and small scale variable should not be transferred to the future climate. Statistical downscaling assumes that the statistical relationships inherent in present climate at local scale will also hold for the future climate (Hillel et al., 2012; Philippe Gachona, 2007). It is not certain whether these small scale interactions observed in present and past climate will hold for the future or not. Therefore, statistical downscaling methods can be misleading to be used under this assumption (Hidalgo et al., 2008; RL. Wilby, 2004).

As the SD methods require database of historical observations, SD methods can only be applied if the database of historical observations is available for the control period. And, it should be paid attention that the records should not contain any unrealistic values, which could result in inaccurate interpretation.

The advantages and disadvantages of SD techniques have different influence on future climate projections, since some techniques are unable to represent the extremes of climate events (Chen et al., 2011). Therefore it must be paid attention to choose the SD techniques which suit best the catchment characteristics.

In this study, Change Factor (also known as delta change method) (Reynard et al., 2001) and Bias Correction In Mean methods are applied to all RCM outputs

given in Table 1.1. The reason of using more than single SD method is due to the fact that SD methods are also potential source of uncertainty in forecasting the climate variables for a hydrological basin, as their weakness and strength are varying due to their different logic.

Table 1.2. Comparative Summary of SD and DD techniques (Adopted from Wilby and Wigley, 1997)

	Statistical Downscaling	Dynamical Downscaling
Advantages	Comparatively cheap and computationally efficient	Produces responses based on physically consistent processes
	Can provide point-scale climatic variables from GCM scale output	Produces finer resolution information from GCM-scale output that can resolve atmospheric processes on a smaller scale
	Can be used to derive variables not available from RCMs	
	Easily transferable to other regions	
	Based on standard and accepted statistical procedures	
	Able to directly incorporate observations into method	
Disadvantages	Require long and reliable observed historical data series for calibration	Computationally intensive
	Dependent upon choice of predictors	Limited number of scenario ensembles available
	Non-stationary in the predictor-predictand relationship	Strongly dependent on GCM boundary forcing
	Climate system feedbacks not included	
	Dependent on GCM boundary forcing: affected by biases in underlying GCM	
	Domain size, climatic region and season affects downscaling skill	

1.2.7. Change factor and Bias Correction in Mean Methods

Change factor (CF) statistical downscaling method is relatively the most straightforward and common method for downscaling as it requires very little effort to apply. Change factor methods can take into accounts different measurements, which are mean only, mean and variance, and Quantile mapping. In this study, only the change factor in mean method is applied.

Change factor statistical downscaling is very commonly used in previous studies on climate change impact assessment. Diaz-Nieto Jacqueline (2005) used CF and another SD method in their paper to compare the impact of both method and they reported that the CF method assumes the climate pattern remain the same in the future climate which means that the properties of present climate data such as variability and range are conveyed to the future. Their findings conclude that temporal sequencing of wet and dry days remains same when CF is used, because the multiplication of change factors clearly cannot change the number of dry and wet days. They mentioned that as a disadvantage of the method. Prudhomme et al. (2002) claimed rightfully that any change in precipitation, increase or decrease, is evenly distributed to the future climate daily rain days. Zahmatkesh et al. (2014), in their study investigating the urban storm water runoff, used CF method to statistically downscale the precipitation to hourly temporal resolution to analyze extreme runoff and flood events. They reported that CF can be classified either additive or multiplicative and stated that multiplicative CF may produce unreliable values (unrealistically small or large values), therefore they used additive CF method for their study. They concluded that using additive CF didn't increase precipitation peak values, instead, it increased average precipitation depth and annual cumulative precipitation prediction considerably. Numerous studies that have implemented CF method to downscale can be found in literature (Anandhi et al., 2011; Chen et al., 2013; P. Willems, 2011; Sunyer et al., 2012)

The mean and variance bias correction firstly proposed by Leander et al. (2007), which considers systematic errors in mean and variance for each day with respect to the control period. In this study, since it can be seen that bias correction might result in unexpectedly large daily runoff values due to its exponential equation, bias correction in only mean method is used. The advantages and disadvantages of bias correction in mean method is given in Table 1.3.

Table 1.3. Advantages and disadvantages of BC in mean method (Adopted from Sunyer, 2014)

Advantages	Disadvantages
Easy to apply	Relies on stationary of transformation parameters, which cannot be verified.
Autocorrelation of the precipitation only weakly affected by non-linear transformation	Does not correct for the length of dry/wet spells
Preserves the sequences of dry/wet days from the RCM simulations, thus can account for the changes in length of dry and wet spells, however, these indexes are not corrected	

1.3. Problem Statement

The contribution by the parameterization of a hydrological model to the uncertainty in the projected changes in high and low flow prediction for the future period has been given less attention as a source of uncertainty. This research focuses on the assessment of uncertainty in the changes in high and low flow prediction for the future period due to two factors; the parameterization of hydrological model and the temperature and precipitation inputs from fifteen different Regional Climate Models from ENSEMBLE Project. The uncertainty due to the precipitation and temperature inputs is investigated by using fifteen different RCMs and also by using two different statistical downscaling (SD) methods, “Bias Correction in Mean” and “Change Factor”, while the uncertainty due to the parameterization of the hydrological model is assessed by using twenty five different parameter sets generated by Monte-Carlo simulation technique using differently tailored Nash functions as the objective function during the calibration of the hydrological model, which are NSE_Normal, NSE_BL, NSE_p3, NSE_Viney and NSE_Weighted. Also, the uncertainty in the occurrence time of high and low flows is investigated by the help of seasonality index.

CHAPTER 2

STUDY AREA, DATA AND MODELS

2.1. Study Area and Data Set

Omerli catchment is located between $29^{\circ} 11' - 29^{\circ} 40'$ latitudes and $40^{\circ} 51' - 41^{\circ} 07'$ longitudes. (Figure 2.1, Figure 2.2), near in Istanbul Province, in Marmara Region. The catchment area is 621 km^2 and dominated by the land cover types of forest (50%), agriculture (25%), lake (2.7%) and settlement (7%). It is a strategically important water basin since it provides water supply especially to the water demand of Istanbul and nearby settlements. It is a natural protected area and home to plenty of endemic plants.



Figure 2.1. Omerli Catchment (Andrew Byfield and Neriman Özhatay, 2009)

Omerli catchment's climate is a transitional climate, affected by the Black Sea from the north, Marmara Sea and Aegean Sea from the south. Consequently, the influence of both maritime and Mediterranean climates can be seen in the basin

area. The two coldest months of the year in terms of lowest monthly average temperature during a 52-year period between 1961 and 2012 are January and February with the monthly average temperature of 5.83°C and 5.97°C, respectively. The two warmest months are July and August with an average temperature of 23.43°C and 23.38°C, respectively. The average annual precipitation in the Omerli Basin is 795.24 mm. December (118.19 mm) and January (97.78 mm) are the two wettest months, while July (27.51 mm) and June (31.54 mm) are the driest months for the Omerli catchment area.

2.2. Observed Data Set

The observed daily precipitation and temperature records for the years 1961-2004 are provided by State Meteorological Service. This period is also referred to as observation period.

The observed discharge records are provided by General Directorate of State Hydraulic Works (GDSHW) for the period 1978-2004 including some missing records. The gauging station is “02-67” in Figure 2.2. The absence of daily observation records within provided 26 years period might decrease the reliability of the findings of this study, unfortunately.

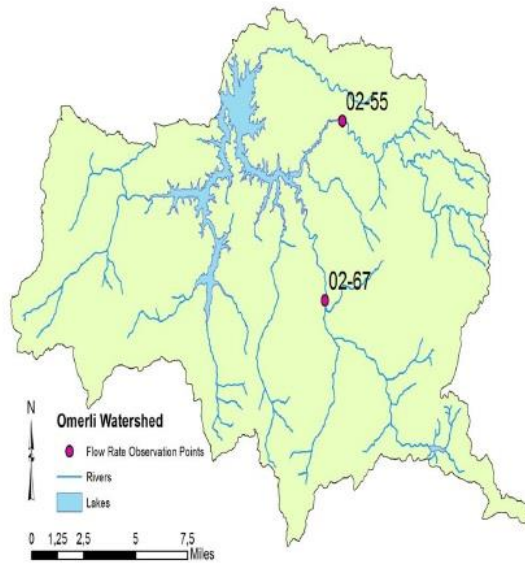


Figure 2.2. Omerli Catchment (I. Yucel, FLOODFREQ Project, 2010)

2.3. Climate Models Data Sets

Daily re-analyzed precipitation and temperature for the period 1961-1990 and the projections of temperature and precipitation for the future period 2071-2099 were obtained from fifteen RCMs with 25 km spatial resolution from the ENSEMBLES project (Van der Linden P. et al., 2009), listed in Table 2.1. All RCMs used in the study were run under A1B emission scenario determined by IPCC in which the world shows rapid economic growth yet maintaining a balance across all sources, i.e. not heavily relying on a particular energy source.

The reason of using fifteen different RCMs driven by six different GCMs is to efficiently reveal the relative uncertainty incurred by the climate projections, without sticking to a single climate model. Because, there might be a case in which a RCM performing well for one catchment performs poorly for another. A RCM performing well for the observed data does not necessarily mean that it will also perform well for the future time, according to Knutti (2010).

Table 2.1. List of RCMs used in the study

RCM NO	Model Acronym	Model	Driving GCM	Institute
1	C4IRCA3	RCA3	HadCM3Q16	Climate Change Consortium Ireland
2	CNRM-RM5.1	ALADIN	ARPEGE	Centre National Meteorology
3	DMI-HIRHAM5	DMI-HIRHAM	ARPEGE	Danish Meteorological Institute
4			ECHAM5	
5			BCM	
6	ETHZ-CLM	CLM	HadCM3Q0	ETH Zürich
7	ICTP-REGCM3	RegCM	ECHAM5-r3	International Centre for Theoretical Physics
8	KNMI	RACMO2	ECHAM5-r3	Royal Netherlands Meteorological Institute
9	METO- HC_HadRM3Q0	HadRM3Q0 (normal sensitivity)	HadRM3Q	Hadley Centre
10	METO- HC_HadRM3Q3	HadRM3Q3 (low sensitivity)	HadCM3Q3	
11	METO- HC_HadRM3Q16	HadRM3Q16 (high sensitivity)	HadCM3Q16	
12	MPI-M-REMO	REMO	ECHAM5-r3	Max-Planck Meteorology Institute
13	SMHIRCA	RCA	ECHAM5-r3	Swedish Meteorological and Hydrological Institute
14			HadCM3Q3	
15			BCM	

2.4. Hydrological Model

In this study, precipitation and temperature inputs are converted into discharge by using the HBV (S. Bergström, 1976; S. Bergström, 1992), which is a numerical rainfall-runoff model for simulating hydrological processes in a catchment scale. It uses daily rainfall, temperature and potential evapotranspiration as input data. In addition to precipitation data, the model uses temperature data to calculate snow melt, snow accumulation and potential

evaporation. It is widely used in the simulation of runoff values for the catchments with the different climate characteristics from all around the world.

CHAPTER 3

METHODOLOGY

The main purpose of this study is to evaluate the probable sources of uncertainty in projected changes of extreme runoff due to two factors: the parameterization of hydrological model and the temperature and precipitation inputs from RCMs. The uncertainty due to the precipitation and temperature inputs is investigated by using fifteen different RCMs and also by using two different SD methods, BC and CF, while the uncertainty due to the parameterization of the hydrological model is assessed by using twenty five different parameter sets generated by Monte-Carlo simulation technique using differently tailored Nash functions as the objective function during the calibration of the hydrological model.

In this chapter, HBV hydrologic model calibration procedure and objective functions used to calibrate it, model performance, methodology for uncertainty assessment and seasonality are given.

3.1. HBV Hydrological Model Calibration

Before making use of the HBV rainfall-runoff model, it is necessary to calibrate the model primarily according to the catchment's characteristics and properties in order to have reliable discharge simulations.

In order to calibrate HBV to Omerli catchment, an R script that implements an automatic parameter estimation procedure (PEST) is used (Lawrence, 2009). By using observed data (precipitation, temperature and discharge), the R script coordinates the calibration of the HBV model with Dynamically Dimensioned Search method (DDS) developed by Tolson and Shoemaker (2007), which is a continuous heuristic global search algorithm for the calibration of multi-

parameter models. DDS automatically searches the different combinations of parameter values and finds the best-possible solutions suitable to represent the catchment, i.e. observed data (Tolson et al., 2007). After DDS implementation, a subsequent Monte-Carlo simulation is applied to derive the reasonable approximations of probability distributions of parameters' value, which requires a large number of simulations (in this case: 1200 model calls). Monte Carlo simulation method is based on repeated many times random sampling to approximate or obtain the distribution of an unknown probabilistic entity (Klukowska, 2014). Monte Carlo simulation is performed by using constricted parameter ranges defined by the 3% of best parameter sets from DDS calibration (Fifteen free parameters calibrated). By doing so, 24 remaining parameter sets for each Nash-Sutcliffe-Efficiency (NSE) function are sampled.

3.1.1. Objective Functions of Calibration

During the calibration process, the optimization algorithm DDS uses one of the five differently tailored types of NSE as the objective function to determine which parameter set is the most suitable one for the catchment in question. NSE is generally used for the hydrologic models to assess their predictive power. Original NSE's equation is defined as:

$$NSE_{Normal} = 1 - \frac{\sum_{t=1}^T (Q_o^t - Q_m^t)^2}{\sum_{t=1}^T (Q_o^t - \bar{Q}_o)^2} \quad (3.1)$$

where Q_o^t and Q_m^t are observed discharge and modeled discharge at time t , respectively. And \bar{Q}_o is the mean observed discharge over the observed period.

The NS efficiency can range from $-\infty$ to 1 . An efficiency of 1 ($E=1$) indicates that the predictive model perfectly matches with the observed data, while an efficiency of 0 ($E=0$) indicates that the mean of the observed data and the predictive model are equally accurate to represent the observed data. And when

the efficiency is less than zero ($E < 0$), it indicates that the observed mean is a better predictor than the developed model.

Beside the original version of the NSE given above (NSE_Normal), four other modified NSEs are used as objective functions during calibration process; which are NSE-BL, NSE-p3, NSE-Viney and NSE-Weighted. Their definitions are given below:

$$NSE_{BL} = NSE - w * \left| \frac{\sum_{t=1}^T (Q_m^t - Q_o^t)}{\sum_{t=1}^T Q_o^t} \right|, w = 0.1 \quad (3.2)$$

$$NSE_{p3} = 1 - \frac{\sum_{t=1}^T (Q_o^t - Q_m^t)^3}{\sum_{t=1}^T (Q_o^t - \bar{Q}_o)^3} \quad (3.3)$$

$$NSE_{Viney} = NSE - 5 * \left| \log \left(1 + \frac{\sum_{t=1}^T (Q_m^t - Q_o^t)}{\sum_{t=1}^T Q_o^t} \right) \right|^{2.5} \quad (3.4)$$

$$NSE_{Weighted} = 1 - \frac{\sum_{t=1}^T Q_o^t (Q_o^t - Q_m^t)^2}{\sum_{t=1}^T Q_o^t (Q_o^t - \bar{Q}_o)^2} \quad (3.5)$$

The important point to make is that our five objective functions differ so that two of them are designed to fit the model against peak flows (i.e. NSE_Weighted, NSE_P3) and the other two (i.e. NSE_Viney, NSE_BL) are designed to estimate an optimal NSE while also minimizing the volumetric bias.

3.1.2 Calibration Procedure

Observed records should be used to calibrate the hydrological model according to the catchment characteristics. Therefore, a “ptq.dta” file containing observed precipitation, temperature and discharge records for the calibration period 01/10/1978 – 30/09/1985 is used. The R script produces 25 different parameter files (i.e. param.dat) optimized for each NSE function mentioned above (125

parameter files in total obtained). Then, the HBV model is executed with each parameter file to model the discharge by using observed precipitation and temperature records for the period 1986-2004, also known as validation period. After the execution is finished, 25 discharge files are generated for each NSE function (thus 125 files in total). These files contain daily “precipitation”, “temperature”, “predicted evaporation”, “snow reserve”, “snow cover”, “soil moisture”, “upper and lower zone”, “qsim” (simulated discharge) and “qobs” (observed discharge) values.

To validate the simulations by parameter files with respect to the observations, three statistical indicators, Root Mean Square Error (RMSE), Pearson Correlation Coefficient (R) and bias are used.

RMSE is a frequently used measure of the difference between the values predicted by a model and the values observed. RMSE’s definition is given below:

$$\text{RMSE} = \sqrt{\frac{\sum_{t=1}^n (Q_o^t - Q_m^t)^2}{n}} \quad (3.6)$$

where Q_o^t and Q_m^t are observed discharge and modeled discharge at time t , respectively. The lower the RMSE value means better fit to the catchment.

The second performance indicator is Pearson correlation coefficient R , which is a correlation coefficient to determine the direction of a linear relationship between predictor and independent variable; in our case, those are model output and observed values. Pearson correlation coefficient can be defined as:

$$r = \frac{\sum_{t=1}^n (Q_o^t - \bar{Q}_o) * (Q_m^t - \bar{Q}_m)}{\sqrt{\sum_{t=1}^n (Q_o^t - \bar{Q}_o)^2 * \sum_{t=1}^n (Q_m^t - \bar{Q}_m)^2}} \quad (3.7)$$

Where Q_o^t and Q_m^t are observed discharge and modeled discharge at time t , and \bar{Q}_o and \bar{Q}_m are the mean observed discharge and mean modeled discharge over the observed period, respectively. The correlation coefficient can range from -1 to $+1$. If it is equal to $+1$, that indicates there is a perfect increasing linear relationship between two variables, while coefficient of -1 implies a perfect decreasing linear relationship. A correlation of coefficient of 0 indicates that there is not any linear relationship between them.

Another model performance indicator is Mean Bias error which is used to detect if the prediction model differs from the observed data in a specific manner or not. It is defined as:

$$\text{Mean bias error} = \frac{1}{n} \sum_{t=1}^n (Q_m^t - Q_o^t) / Q_o^t \quad (3.8)$$

Mean bias error is simply the difference between the observed and the modeled values. Thus, the model accuracy can be said to decline when mean bias error moves away from zero. If it is positive or negative, the model can be said to overestimate or underestimate values, respectively.

3.2. Multi Decision Making Method- TOPSIS

“Technique for Order of Preference by Similarity to Ideal Solution” (TOPSIS) is a compensatory method, by allowing trade-offs between decision criteria so that a poor results obtained from a criteria can be compensated by another (Jamal Khosravi, 2011). TOPSIS was originally developed by Hwang and Yoon in 1981 and improved further by Yoon in 1987 and by Hwang, Lai and Liu in 1993. A multi decision making method was essential to use because there could be a RCM with greater NSE and correlation coefficient R, on the other hand greater RMSE and the bias, which makes it difficult to determine whether a RCM is a better choice for the catchment comparing to others.

Since we have 4 different performance indicators (NSE, RMSE, R and Bias):

1. TOPSIS is applied to sort RCMs in descending order of their ability to reproduce the precipitation for the reference period.
2. TOPSIS is applied to sort simulations by parameter files for the reference period by their TOPSIS Grades

It is based on the idea that an “alternative which has the shortest geometric distance to the ideal solution and the longest geometric distance from the non-ideal solution has highest grade” and therefore, it is determined as the best choice (Hwang et al., 1993). The more similar option to the ideal solution, the higher grade it has, therefore it is more likely for the option to be determined as the best choice. Each criterion is assigned a relative weight that signifies the relative importance in proportion to the other criteria, and the values of criteria during the evaluation of alternatives are normalized before the calculation of solution.

$$s. t. \sum_{i=1}^4 w_i = 1 \quad 0 \leq w_i \leq 1 \quad (3.9)$$

3.3. Statistical Downscaling Methods

3.3.1. Change Factor Method

The monthly precipitation changes of a climate model are calculated by proportioning monthly averaged precipitation values from future and control period. Afterwards, these change factors determined for every month are applied to observed data.

CF for precipitation and temperature equation is given below:

$$CFP_j = \frac{RCM_j^{Future}}{RCM_j^{Reference}} \quad j = 1 \dots 12 \quad (3.10)$$

where RCM_j^{Future} and $RCM_j^{Reference}$ is the monthly averaged precipitation of future time series and control time series, respectively.

This factor is applied to the observed daily precipitation records of the control period.

$$P_{i,j}^{Downscaled} = P_{i,j}^{Observed} * CFP_j \quad i = 1 \dots 30, j = 1 \dots 12 \quad (3.11)$$

To find the change factors for the temperature, the difference in monthly averaged temperature are calculated for each month. Equation (3.7)

$$CFT_j = RCM_j^{Future} - RCM_j^{Reference} \quad j = 1 \dots 12 \quad (3.12)$$

For the downscaling of temperature, change factors are simply added to the observed daily records.

$$T_{i,j}^{Downscaled} = T_{i,j}^{Observed} + CFT_j \quad i = 1 \dots 30, j = 1, \dots 12 \quad (3.13)$$

3.3.2. Bias Correction in Mean Method

For every day in a year ($j=1 \dots 365-366$), 61 days centred on day j (30 days before and after the day j) from all years for observed data and for a RCM output for the reference period are formed. Let's denote these subsets for each RCM as following: $P_{.,j}^{Observed}$ and $P_{.,j}^{Reference}$ respectively:

Calculate a_j , where:

$$a_j = \frac{1}{n} \sum_{t=1}^n P_{t,j}^{Observed} / \frac{1}{n} \sum_{t=1}^n P_{t,j}^{Reference} \quad j = 1 \dots 365 \text{ or } 366 \quad (3.14)$$

Where n is equal to 61.

And finally the set of a_j estimated for every day in a year is applied to the future series as given below:

$$P_{t,j}^{Corrected} = (a_j * P_{t,j}^{RCM-Future})^{b_j} \quad j = 1 \dots 365 \text{ or } 366 \quad (3.15)$$

where b_j equals to 1 for BC in mean.

3.4. Extreme Value Series

Independent extreme high flow discharges are extracted from the series through Peak Over Threshold (POT) method. POT method uses a predefined T-year return level for the number of high flows that will be included in the series for a given period of time. For example, with a 30-year record, 30 most extreme and independent events will be included in the analysis for the 1-year return period, whereas for the 5-year return period 6 most extreme and independent events will be extracted. The events must satisfy the independence criteria set by Willems (2009) to make sure that the events extracted from the series are independent to each other, not the residual of another. For the precipitation independency, the extreme events can be classified as independent if and only they are separated by more than X days, where the value of X is set equal to the aggregation time (search window). For the extreme discharge independency criteria, it is applied an inter-event level criterion as an addition to the inter-event time. In this study, the independency criteria from the WETSPRO is adopted. Two successive high flows are considered nearly independent when the following three conditions are satisfied, according to the WETSPRO, Willems (2004):

- The time between the two events exceeds a time $k=4$
- Base flow between the two high flows becomes smaller than a fraction ($f=0.7$) of the lower of the two high flows.
- the discharge increment between high flow and minimum flow between the two events is higher than a threshold $q=3 \text{ m}^3 \text{ s}^{-1}$

For the low flow selection, the events lower than the value of 20 percentile of the data are selected as the low extreme events.

3.5. Uncertainty Assessment

Total variance calculated in this study as a measure for uncertainty in the changes in projected extreme discharge consists of two variances: variance from climate projections, and variance from hydrological parameterization. The equation for the calculation of total variance is shown in Equation 3.16:

$$\bar{\sigma}^2_{total\ variance} = \bar{\sigma}^2_{RCM} + \bar{\sigma}^2_{HP} \quad (3.16)$$

where $\bar{\sigma}^2_{RCM}$ and $\bar{\sigma}^2_{HP}$ are the fractional variance explained by climate projection models and fractional variance explained by hydrological parameterization.

Fractional variance in the high and low discharge explained by hydrological model parameterization calculation is as follows: By using the daily precipitation and temperature data from three data types; Original RCMs, bias corrected (with downscaling) series by BC and CF; HBV Model is run with using all parameter files for the future and the reference period. The POT series are extracted from the simulations for both periods:

$$P_{k,m,j}^{Reference} \text{ and } P_{k,m,j}^{Future} \quad k = 1 \dots 15, m = 1 \dots 5, j = 1 \dots 25 \quad (3.17)$$

where k , m and j stands for the set of RCMs, NSE functions and parameter files, respectively. The average of the high flows is calculated and represented as below for a given set of high flows (p_i) in a POT series $P_{k,m,j}$:

$$\bar{P}_{k,m,j} = \frac{1}{n} * \sum_{i=1}^n p_i \quad (3.18)$$

The absolute difference between $\bar{P}_{k,m,j}^{Future}$ and $\bar{P}_{k,m,j}^{Reference}$ is calculated and represented as below:

$$\Delta P_{k,m,j} = |\bar{P}_{k,m,j}^{Future} - \bar{P}_{k,m,j}^{Reference}| \quad (3.19)$$

Finally, mean variance explained by hydrological parameterization is calculated for every NSE function as follows:

$$\bar{\sigma}_{HP,m}^2 = \frac{1}{15} \sum_{k=1}^{15} \frac{\sum_{j=1}^{25} (\Delta P_{k,m,j} - \Delta \bar{P}_{k,m,1:25})^2}{25} \quad (3.20)$$

As for the fractional mean variance explained by climate projection models, the Equation 3.21 is executed:

$$\bar{\sigma}_{RCM,m}^2 = \frac{1}{25} \sum_{j=1}^{25} \frac{\sum_{k=1}^{15} (\Delta P_{k,m,j} - \Delta \bar{P}_{1:15,m,j})^2}{15} \quad (3.21)$$

Finally, the sum of two mean variances (Equation 3.16) stands for the measure of uncertainty and allows user to assess the relative contribution of hydrological model parameterization to the uncertainty in uncertainty in the changes in projected extreme flows.

3.6. Seasonality

Changes in flood seasonality is calculated to understand if the different SD methods have an influence on the assessment of seasonality inherent in the basin. The factor S_D is calculated for two SD methods and Original RCMs for both reference and future periods and plotted as notched box plot. It is calculated as follows:

$$S_D = \frac{POT_{Sep-Feb}}{POT_{all}} - \frac{POT_{Mar-Aug}}{POT_{all}} \quad (3.22)$$

where $POT_{Sep-Feb}$ and $POT_{Mar-Aug}$ are the POT analysis of extreme events for 6-month periods from September to February and from March to August, respectively, while POT_{all} is the list of POT high flow events for the whole series. S_D can range from -1 to +1 and negative coefficients indicate most high flow events occurring in spring/summer, where positive numbers indicate dominant high flows in autumn/winter.

3.7. Organizing Essential Data

To be able to do the analysis mentioned above, it is needed to undergone serious computational effort. HBV Model has been run for $15 \times 125 \times 2 \times 3 = 11250$ times (the number of RCMs * the number of parameter files * the number of periods * three major data set: Original RCM, BC and CF) to obtain the hydrological discharge outputs. Therefore, enormous effort has been paid to handling the data.

CHAPTER 4

PRECIPITATION ANALYSIS

4.1. Evaluation of RCMs precipitation

In this subsection, the performance of RCMs-derived daily precipitation is briefly evaluated for the period 1961-1990. A more detailed performance evaluation of these RCMs that accounts for extreme precipitation over different seasons in Omerli Basin can be found in Kara (2014). Their RMSE, NSE, Correlation Coefficient R and Bias measures of 15 RCMs in deriving daily precipitation are shown in Figure 4.1.

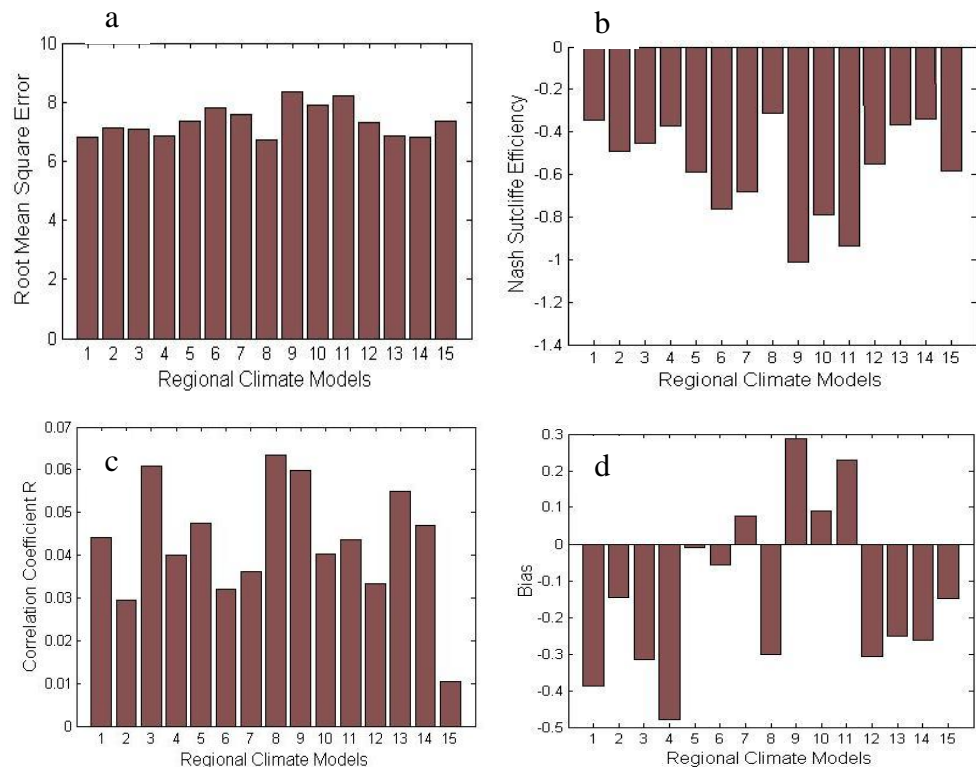


Figure 4.1 - RMSE, NSE, Correlation Coefficient R and Bias measures of 15 RCMs in deriving daily precipitation

As the lower the RMSE value means better fit to the catchment, it can be observed that RCMs' RMSE values are similar, yet fair (Figure 4.1-a).

An efficiency of 1 indicates that the predictive model perfectly matches with the observed data, while an efficiency of zero ($E=0$) indicates that the mean of the observed data and the predictive model are equally accurate to represent the observed data. The bar chart indicates that "observed mean" is a better predictor than the RCMs, as the efficiencies are less than zero (Figure 4.1-b).

If R is equal to one, that indicates that there is a perfect increasing linear relationship between two variables, while an R that is equal to zero indicates that there is not any linear relationship between them. Therefore the RCM 8, 3, 9, and 13, which outperforms the other RCMs in terms of R, have a slight increasing linear relationship with the observed data (Figure 4.1-c).

It can be observed that there is a tendency to underestimate the precipitation by RCMs for the reference period. The model accuracy can be said to decline when mean bias error moves away from zero, therefore the bar chart indicates that the RCM 7, 9, 10 and 11 overestimate the precipitation for the period 1961-1990, whereas the others underestimate (Figure 4.1-d).

Table 4.1. RCM's performance indicators for the reference period 1961 -1990

RCM NO	RMSE	NSE	R	BIAS
1	6.831	-0.344	0.044	-0.388
2	7.145	-0.490	0.030	-0.145
3	7.062	-0.456	0.061	-0.314
4	6.858	-0.373	0.040	-0.479
5	7.372	-0.586	0.048	-0.010
6	7.816	-0.761	0.032	-0.057
7	7.591	-0.682	0.036	0.076
8	6.704	-0.312	0.063	-0.302
9	8.360	-1.014	0.060	0.287
10	7.878	-0.788	0.040	0.090
11	8.196	-0.936	0.044	0.229
12	7.287	-0.550	0.033	-0.306
13	6.848	-0.369	0.055	-0.253
14	6.813	-0.338	0.047	-0.263
15	7.365	-0.584	0.010	-0.150

It can be seen that even the best RCM outputs do not seem sufficient to fully represent Omerli catchment's spatial precipitation pattern, as their performance indicators are poor overall. However, it can be observed from the Figure 4.5 that all RCMs are able to capture the seasonal precipitation pattern very well, which is wet autumn & winter and semi-dry spring & dry summer.

If it is asked to choose some of the best performing RCMs or sort them according to their ability to reproduce the precipitation pattern for the period 1961-1990, it may be necessary to use one of the multi criteria decision method in order to do that, however, all of RCMs are used in this thesis for the uncertainty assessment.

The table of weights assigned to each criterion is given in Table 4.1.:

Table 4.2. The Weights assigned to criteria

NSE	w ₁	0.30
RMSE	w ₂	0.30
Coer.Coef. R	w ₃	0.30
Bias	w ₄	0.1
	Total Weight	1

After the implementation of TOPSIS method, sorted RCMs based on TOPSIS Grades were given in Table 4.2.

Table 4.3. Sorted RCMs based on TOPSIS Grades

RCMs	TOPSIS Grade
8	0.82
13	0.80
3	0.76
14	0.74
5	0.68
1	0.67
4	0.61
2	0.56
7	0.52
12	0.52
10	0.49
9	0.48
6	0.45
11	0.41
15	0.40

Table 4.2 shows that RCM 8 and RCM 15 are the most and least successful RCM in reproducing the precipitation pattern for the period 1961-1990, respectively.

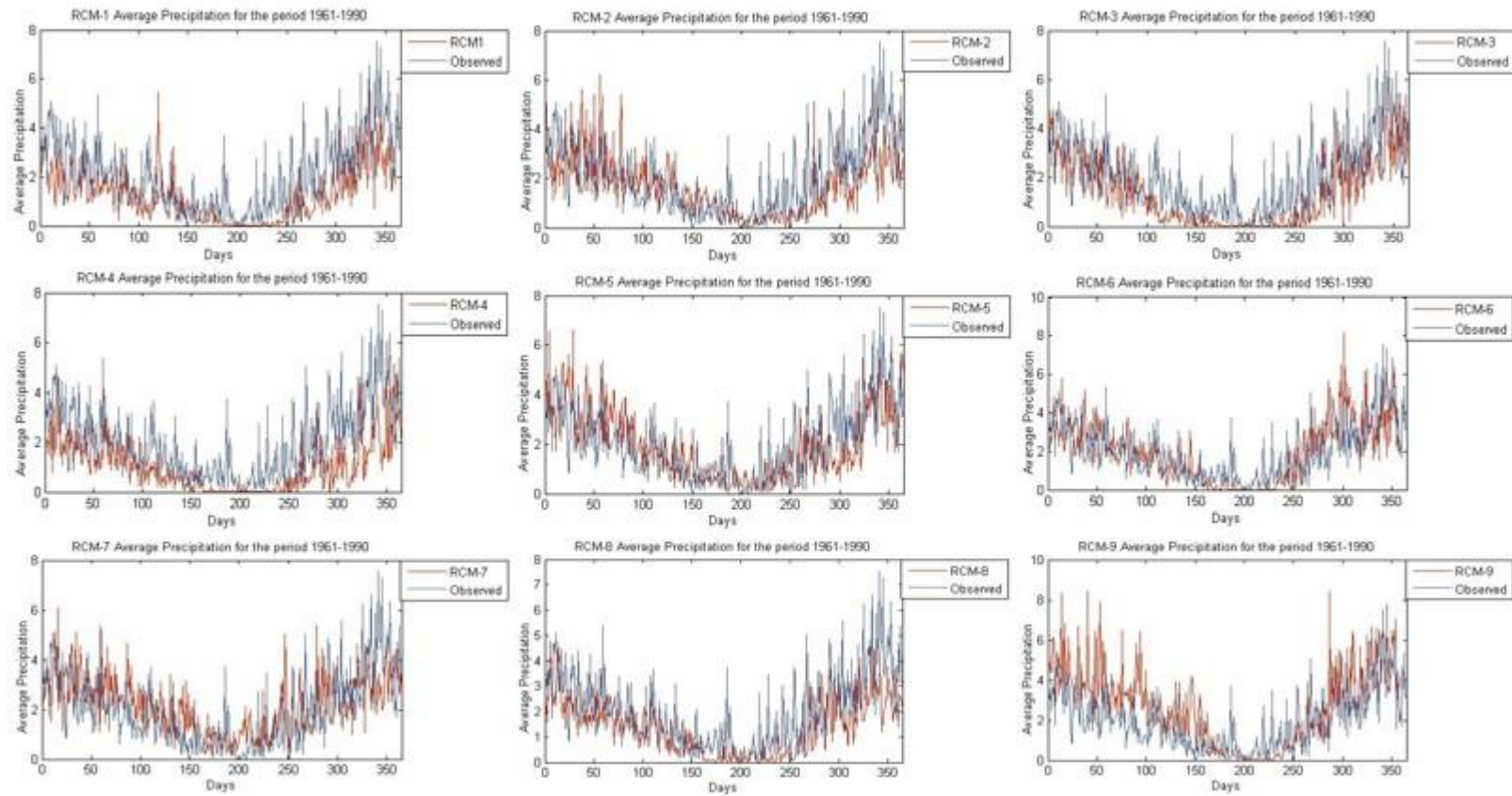


Figure 4.2. Averaged daily precipitation of RCMs for the period 1961-1999

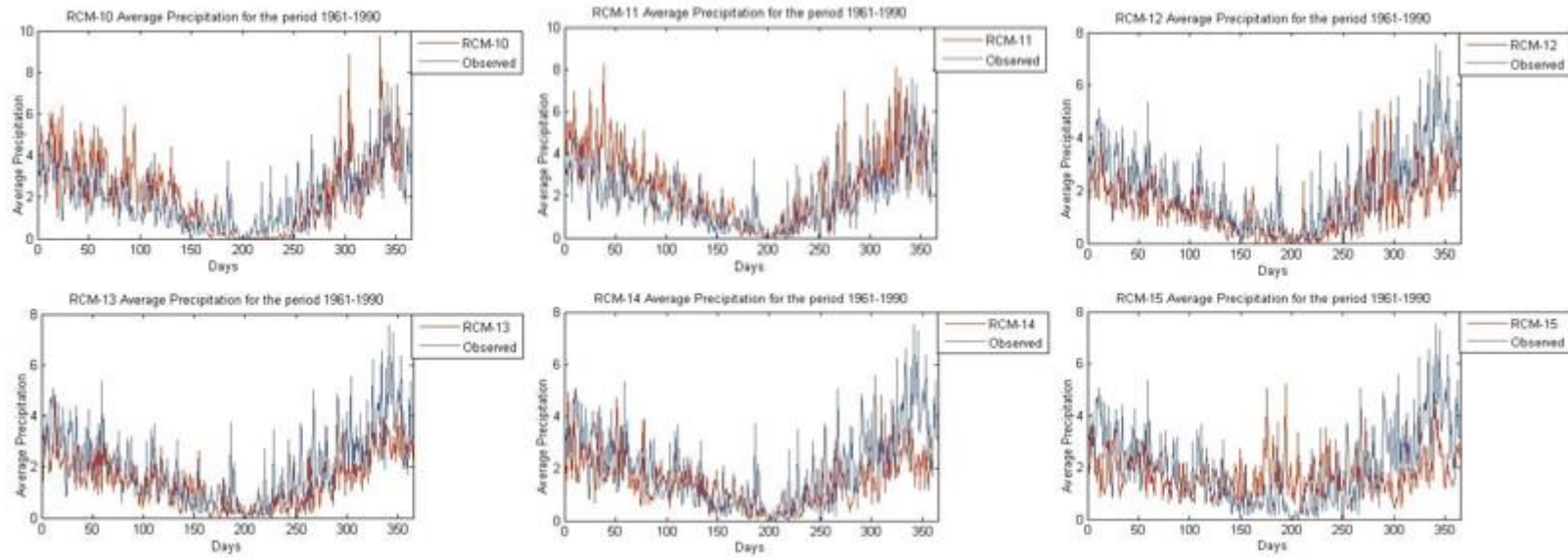


Figure 4.2. Cont.

CHAPTER 5

RESULTS and DISCUSSION

5.1. Hydrological Model Calibration

HBV Model is calibrated by using observed daily precipitation, temperature and discharge records for the period 1978-1985. As mentioned in previous Chapter 3, 25 parameter files are sampled for each of five NSE functions.

5.2. Evaluation of HBV Calibration for the period 1986-2004

HBV Model is run with 25 parameter files for each NSE function for the period 1986-2004 to validate the calibration results.

Figure 5.1 displaying simulated and observed discharges for the period 1986-2004 is given. Each box in the boxplot contains HBV simulations using observed data due to the corresponding 25 parameter files. It is hard to interpret the boxplot showing discharge values, as the outliers are far greater than the Quartiles. It can be observed that there are considerable number of high flow events depicted by the red dots as outliers in all NSE results and also in observation. Except for NSE_p3, which was an anticipated results as the NSE_p3 is especially designed to estimate the extreme events, the other NSE functions are in agreement with the observed data. Table 5.1 shows the performance indicators of each parameter file for the discharge for the validation period 1986-2004.

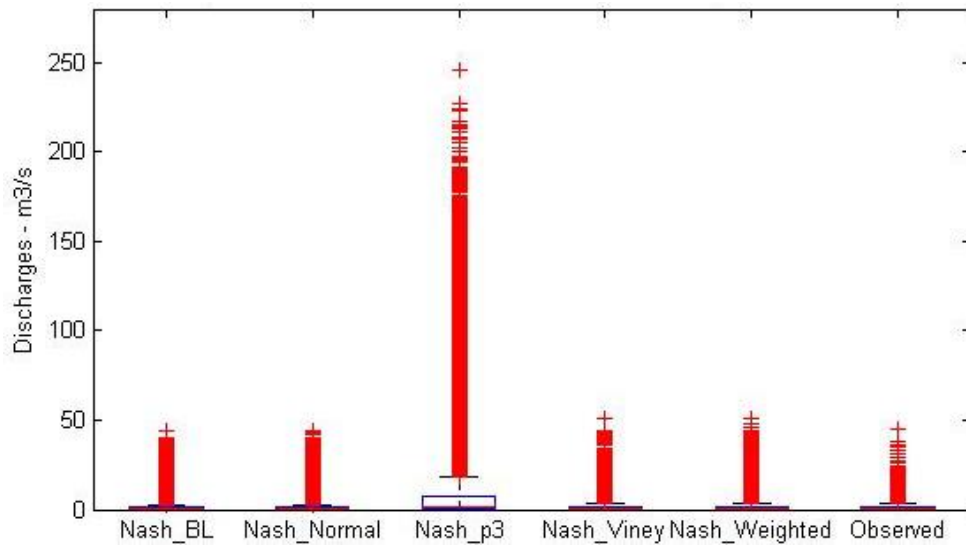


Figure 5.1. Boxplot of simulated and observed discharges for the period 1986-2004

Table 5.1 Performance indicators for the parameter sets for validation period 1986-2004 (Green and red backcolor indicate the best and worst values in each criterion)

P_No	Nash Functions																			
	BL	Normal	P3	Viney	Weighted	BL	Normal	P3	Viney	Weighted	BL	Normal	P3	Viney	Weighted	BL	Normal	P3	Viney	Weighted
	RMSE					NSE					R					Bias				
1	1.37	1.39	11.95	1.39	1.38	0.43	0.41	-42.4	0.41	0.42	0.66	0.67	0.58	0.66	0.68	-0.21	-0.32	5.11	-0.24	-0.14
2	1.43	1.41	10.47	1.4	1.57	0.38	0.39	-32.4	0.41	0.25	0.63	0.64	0.56	0.66	0.63	-0.15	-0.12	4.11	-0.21	0.3
3	1.39	1.45	9.66	1.39	1.56	0.42	0.36	-27.4	0.42	0.26	0.66	0.62	0.57	0.66	0.64	-0.26	-0.27	3.99	-0.03	0.3
4	1.46	1.48	9.5	1.44	1.54	0.35	0.33	-26.5	0.37	0.28	0.61	0.63	0.56	0.64	0.66	-0.29	-0.47	3.77	-0.07	0.05
5	1.43	1.42	11.09	1.48	1.45	0.38	0.38	-36.4	0.33	0.36	0.63	0.64	0.55	0.6	0.65	-0.23	-0.27	4.55	-0.27	-0.13
6	1.48	1.4	9.87	1.42	1.6	0.33	0.41	-28.6	0.39	0.22	0.6	0.64	0.57	0.64	0.66	-0.29	-0.09	3.93	-0.28	0.26
7	1.46	1.41	9.52	1.54	1.43	0.35	0.39	-26.6	0.28	0.38	0.66	0.65	0.55	0.55	0.65	-0.05	-0.26	3.89	-0.31	-0.2
8	1.41	1.44	9.04	1.41	1.59	0.4	0.37	-23.8	0.4	0.23	0.65	0.64	0.58	0.63	0.67	-0.06	-0.09	3.57	-0.06	0.04
9	1.46	1.47	10.73	1.42	1.4	0.35	0.34	-34.1	0.39	0.4	0.64	0.61	0.56	0.64	0.65	-0.46	-0.19	4.98	-0.09	-0.19
10	1.53	1.47	10.59	1.42	1.54	0.29	0.35	-33.1	0.39	0.28	0.62	0.59	0.53	0.64	0.63	-0.55	-0.02	4.93	-0.27	0.06
11	1.43	1.47	8.72	1.54	1.38	0.38	0.34	-22.1	0.28	0.42	0.66	0.61	0.59	0.54	0.65	-0.32	-0.07	3.5	-0.21	-0.17
12	1.45	1.47	10.19	1.42	1.58	0.36	0.34	-30.6	0.39	0.24	0.63	0.62	0.55	0.65	0.64	-0.38	-0.37	4.32	-0.07	0.1
13	1.41	1.49	8.8	1.46	1.38	0.39	0.33	-22.6	0.36	0.42	0.64	0.62	0.55	0.64	0.67	-0.14	-0.45	3.96	-0.38	-0.16
14	1.44	1.42	9.86	1.49	1.46	0.37	0.38	-28.6	0.32	0.35	0.63	0.64	0.59	0.58	0.63	0.02	0.01	4.33	-0.25	-0.13
15	1.45	1.49	8.53	1.45	1.6	0.36	0.33	-21.1	0.36	0.22	0.63	0.61	0.58	0.61	0.63	-0.15	-0.38	3.51	-0.13	0.25
16	1.46	1.46	8.67	1.56	1.62	0.35	0.35	-21.9	0.26	0.2	0.62	0.64	0.62	0.65	0.63	-0.29	-0.37	3.74	-0.08	0.13
17	1.45	1.48	8.88	1.5	1.44	0.36	0.33	-23	0.31	0.37	0.63	0.61	0.57	0.67	0.65	-0.22	-0.38	3.95	0.07	-0.22
18	1.48	1.45	8.2	1.4	1.56	0.33	0.36	-19.5	0.4	0.26	0.62	0.63	0.6	0.66	0.65	-0.42	-0.2	3.21	0.01	0.09
19	1.48	1.47	10.39	1.47	1.51	0.34	0.34	-31.9	0.34	0.31	0.62	0.6	0.61	0.62	0.65	-0.44	-0.22	4.59	-0.36	-0.02
20	1.44	1.47	9.5	1.53	1.44	0.37	0.35	-26.4	0.29	0.37	0.64	0.63	0.57	0.58	0.65	-0.39	-0.25	4.35	-0.27	-0.22
21	1.44	1.47	9.25	1.54	1.48	0.37	0.34	-25	0.28	0.33	0.66	0.6	0.57	0.62	0.65	-0.02	-0.22	4.16	-0.1	-0.2
22	1.47	1.49	9.91	1.57	1.54	0.35	0.32	-28.9	0.25	0.28	0.62	0.58	0.56	0.52	0.63	-0.26	-0.18	4.34	0.01	0.17
23	1.53	1.47	8.31	1.5	1.56	0.29	0.34	-20	0.32	0.26	0.55	0.62	0.62	0.62	0.65	-0.28	-0.36	3.57	-0.09	0.14
24	1.43	1.48	9.68	1.51	1.6	0.38	0.33	-27.5	0.31	0.22	0.66	0.62	0.55	0.66	0.62	-0.14	-0.38	3.83	-0.02	0.08
25	1.5	1.48	8.27	1.51	1.77	0.32	0.33	-19.8	0.31	0.05	0.62	0.61	0.6	0.67	0.56	-0.4	-0.32	3.57	-0.17	0.59

TOPSIS method is implemented to decide which parameter sets calibrated through different NSE function put on best performance in reproducing stream flow for the period 1986-2004. The results in Table 5.2 demonstrated that while NSE_p3 showed worst performance in reproducing discharge values, to some extent the others reproduced stream flow similar to each other.

Table 5.2. Averaged performance indicators of 25 parameter files for each NSE function

NSE Functions	RMSE	NSE	R	BIAS
NSE_BL	1.451	0.360	0.632	-0.255
NSE_Normal	1.456	0.354	0.623	-0.250
NSE_p3	9.583	-27.200	0.574	4.070
NSE_Viney	1.450	0.360	0.665	-0.205
NSE_Weighted	1.519	0.295	0.643	0.031

Table 5.3 gives the parameter files sorted by TOPSIS Grades from best to worst in reproducing the stream flow for the period 1986-2004.

Table 5.3. Sorted parameter files with respect to the TOPSIS Grades

Viney	Param_3	1.000	Normal	Param_10	0.998	Normal	Param_21	0.997	Normal	Param_12	0.996	p3	Param_18	0.534
Viney	Param_18	0.999	BL	Param_15	0.998	Normal	Param_3	0.997	Viney	Param_20	0.995	p3	Param_25	0.526
BL	Param_8	0.999	Weighted	Param_7	0.998	BL	Param_22	0.997	Normal	Param_24	0.995	p3	Param_23	0.522
Normal	Param_6	0.999	Weighted	Param_14	0.998	Viney	Param_25	0.997	Viney	Param_11	0.995	p3	Param_15	0.496
Viney	Param_8	0.999	Viney	Param_1	0.998	BL	Param_11	0.997	Normal	Param_17	0.995	p3	Param_16	0.479
Viney	Param_12	0.999	Normal	Param_11	0.998	Normal	Param_22	0.997	Normal	Param_15	0.995	p3	Param_11	0.472
Normal	Param_14	0.999	BL	Param_3	0.997	BL	Param_16	0.996	Weighted	Param_12	0.995	p3	Param_13	0.462
Weighted	Param_1	0.999	Weighted	Param_17	0.997	BL	Param_4	0.996	BL	Param_23	0.995	p3	Param_17	0.452
Viney	Param_9	0.999	Weighted	Param_20	0.997	Weighted	Param_4	0.996	Weighted	Param_8	0.995	p3	Param_8	0.433
BL	Param_21	0.999	BL	Param_5	0.997	Weighted	Param_10	0.996	Viney	Param_22	0.995	p3	Param_21	0.405
Weighted	Param_13	0.998	Normal	Param_18	0.997	Viney	Param_5	0.996	BL	Param_25	0.995	p3	Param_20	0.372
Normal	Param_2	0.998	Normal	Param_7	0.997	Viney	Param_21	0.996	BL	Param_18	0.995	p3	Param_4	0.371
BL	Param_14	0.998	BL	Param_17	0.997	Viney	Param_14	0.996	BL	Param_19	0.995	p3	Param_7	0.369
Viney	Param_4	0.998	Viney	Param_10	0.997	BL	Param_6	0.996	BL	Param_9	0.995	p3	Param_3	0.350
Weighted	Param_11	0.998	Viney	Param_23	0.997	Weighted	Param_22	0.996	Viney	Param_7	0.995	p3	Param_24	0.347
BL	Param_13	0.998	Viney	Param_24	0.997	Normal	Param_25	0.996	Weighted	Param_3	0.995	p3	Param_14	0.322
Normal	Param_8	0.998	Weighted	Param_19	0.997	Viney	Param_16	0.996	Weighted	Param_24	0.995	p3	Param_6	0.322
BL	Param_24	0.998	Viney	Param_17	0.997	BL	Param_20	0.996	Normal	Param_13	0.995	p3	Param_22	0.316
BL	Param_7	0.998	Normal	Param_5	0.997	Viney	Param_13	0.996	Weighted	Param_2	0.995	p3	Param_12	0.275
BL	Param_2	0.998	Viney	Param_6	0.997	Normal	Param_16	0.996	Normal	Param_4	0.995	p3	Param_19	0.246
Weighted	Param_9	0.998	Normal	Param_9	0.997	Weighted	Param_18	0.996	Weighted	Param_15	0.994	p3	Param_2	0.234
BL	Param_1	0.998	Weighted	Param_21	0.997	BL	Param_12	0.996	Weighted	Param_6	0.994	p3	Param_10	0.216
Viney	Param_2	0.998	Normal	Param_20	0.997	Normal	Param_23	0.996	Weighted	Param_16	0.994	p3	Param_9	0.195
Weighted	Param_5	0.998	Normal	Param_1	0.997	Viney	Param_19	0.996	BL	Param_10	0.993	p3	Param_5	0.140
Viney	Param_15	0.998	Normal	Param_19	0.997	Weighted	Param_23	0.996	Weighted	Param_25	0.989	p3	Param_1	0.001

In order to examine the influence of hydrological model parameterization on reproducing the extreme discharge for the reference period, Peak over Threshold (POT) analysis is carried out to obtain Extreme Value series.

Figure 5.2 displays the POT series collected from the simulation results of 25 parameter files using observed data for each NSE function. The result indicates that except for NSE-p3 which overestimate the high flows, the parameter files calibrated through other NSE functions slightly underestimate the high flows in comparison with observed high flows for the period 1986-2004. NSE_Weighted parameter sets seem to be the best in reproducing the high flow events for the period 1986-2004.

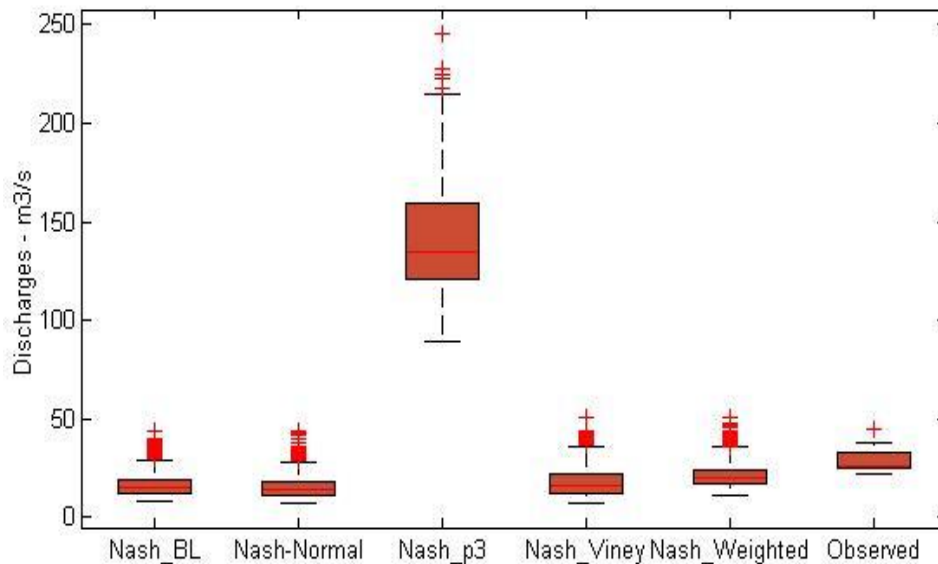


Figure 5.2. Boxplot of simulated and observed high flow discharges for the period 1986-2004

Figure 5.3 indicates that the all parameter files calibrated through each NSE function slightly overestimate the low events compared to the observed low flows for the period 1986-2004. For NSE-p3, NSE-BL and NSE_Viney, it can be seen considerable number of outliers exceed the adjacent values belonging to the corresponding boxes. As in reproducing the extreme high flow event, NSE_Weighted parameter sets seem to be the best in reproducing the low events for the period 1986-2004.

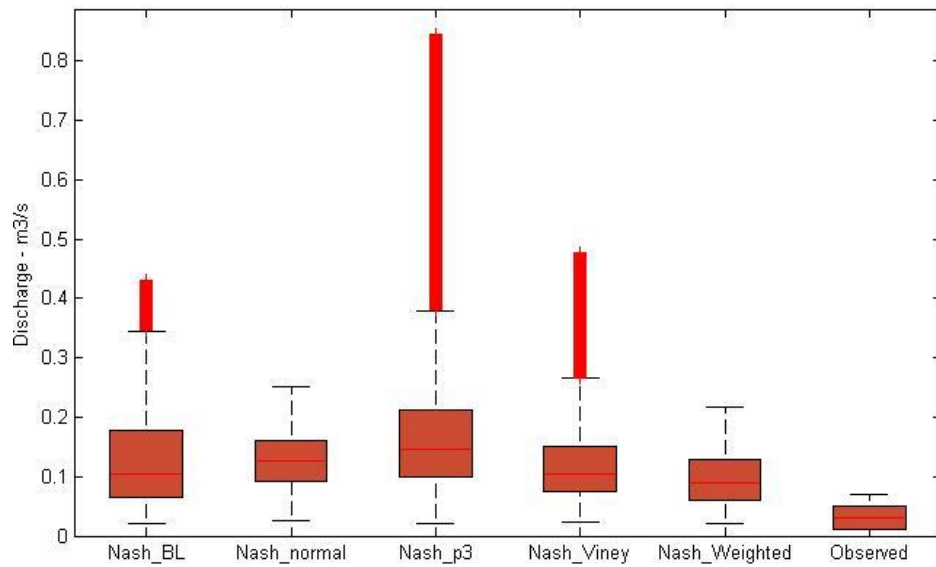


Figure 5.3. Boxplot of simulated and observed low flow for the period 1986-2004

5.3. Uncertainty Analysis for Runoffs from Reference To Future Periods

5.3.1. Uncertainty in High Flow Prediction

Table 5.4 presents the total mean variances in the changes in high flow events from reference to future period among RCMs and hydrological model parameters which are obtained by using downscaled and original precipitation and temperature records. Table 5.4 indicates that the statistical downscaling via CF and “Bias correction in mean” increase the total mean variance in the changes in high flow events from reference to future period, which is similar to the findings in Dobler et al. (2012) in which they reported that the bias correction have great influence on extreme river flows prediction. This could stem from the multiplication process in the implementation of two SD methods. NSE_p3 outputs show substantially greater mean variance among other NSE functions.

Table 5.4. Calculated mean variances among RCMs (Var_RCM) and hydrological model parameters (Var_Hydro) for high flows obtained through downscaled and no downscaled precipitation and temperature

		NSE Functions				
		BL	Normal	p3	Viney	Weighted
Original	Var_Hydro	0.76	1.05	27.48	1.12	0.57
RCMs	Var_RCM	1.92	2.30	53.46	2.33	2.63
Bias Correction in Mean	Var_Hydro	2.19	1.72	45.23	4.04	2.49
	Var_RCM	5.59	5.62	172.81	7.87	9.57
Change Factor	Var_Hydro	4,20	4,49	122,84	8,08	3,51
	Var_RCM	6,66	6,25	496,98	8,06	12,73

Table 5.4 shows that total mean variance for each NSE functions reaches its highest values in CF method. This means that change factor method produces greater variance (therefore, cause more uncertainty) in high flow runoff prediction compared with BC.

Figure 5.4 shows the fractional variance by two uncertainty sources; variance from different hydrological parameterization (HP) and variance from different RCMs. Three charts in Figure 5.4 indicate that the hydrological parameterization comprises a small part of uncertainty relative to the uncertainty explain by RCMs, as these findings comply with the findings in the study of Wilby et al. (2006). HP fractional variance shows a decrease in three NSE functions (NSE_BL, NSE_Normal, NSE_p3) by the simulations using BC data, while it shows an increase in other two NSE functions (NSE_Viney, NSE_Weighted). HP fractional variance shows a decrease in NSE_p3 by the simulation using CF data, while it shows an increase in the rest. Therefore, it can be inferred to some extent there is no consistent effect of SD on the fractional variances explained by two factors. However, both SD methods for three NSE functions (NSE_p3, NSE_Viney, NSE_Weighted) show the same trend in which NSE_p3 decreases HP fraction while NSE_Viney and NSE_Weighted increase HP fraction after the application of both SD. Overall CF becomes more sensitive to HP uncertainty.



Figure 5.4. The fractions of total variance as a measure for uncertainty in the change in mean high flow events due to HP and RCMs

One handicap of comparing CF to BC in mean as SD methods is that CF statistically downscales only the future period, while Bias correction can remove the systematic bias from both period, while downscaling. This difference can prevent CF producing reliable result used in comparison, since Original RCMs' precipitation and temperature reproductions are used to obtain hydrological model outputs for each parameter set for the reference period in evaluating the Delta POTs in the fractional variance calculation for CF method (in other words, simulations using Original RCMs outputs for reference period are used as reference period of CF, too), which is consistent with the procedure used for CF reference period in Dobler et al. (2012).

5.3.2. Uncertainty in Low Flow Prediction

Table 5. presents the total mean variances in the changes in low flow events from reference to future period among RCMs and hydrological model parameters which are obtained by using downscaled and original precipitation and temperature records. In the uncertainty assessment in low flow prediction for the future period, it is faced with the same situation as in high flow prediction. Table 5.5 indicates that the statistical downscaling via CF and “Bias correction in mean” increase the total mean variance. NSE_p3 outputs show greater mean variance among other NSE function.

Table 5.5. Calculated mean variances among RCMs (Var_RCM) and hydrological model parameters (Var_Hydro) for low flows obtained through downscaled and no downscaled precipitation and temperature

		NSE Functions				
		BL	Normal	p3	Viney	Weighted
Original RCMs	Var_Hydro	0.000051	0.000030	0.000073	0.000045	0.000031
	Var_RCM	0.000051	0.000037	0.000096	0.000042	0.000028
Bias Correction in Mean	Var_Hydro	0.000117	0.000054	0.000190	0.000103	0.000069
	Var_RCM	0.000206	0.000171	0.000730	0.000195	0.000154
Change Factor	Var_Hydro	0.001041	0.001086	0.001291	0.000856	0.000826
	Var_RCM	0.000252	0.000296	0.000688	0.000245	0.000175

Table 5.5 shows that total mean variance in low flow prediction by every NSE functions reaches its highest values in CF method, as in high flow prediction. This means that change factor method produces greater variance in extreme event prediction compared with BC. This is a pretty much anticipated result and due to the usage of same output sets as $\bar{P}_{k,m,j}^{Reference}$ during the calculation of $\Delta P_{k,m,j}$.

Figure 5.5 demonstrates that the relative contribution to the uncertainty by HP and RCMs differs between high flow and low flow prediction. The relative contribution to the uncertainty by HP is increased for each NSE function in the simulations using

Original RCM, BC and CF when compared to the relative uncertainty in high flow projections (Figure 5.5 compared to Figure 5.4).



Figure 5.5. The fractions of total variance as a measure for uncertainty in the change in mean low events due to HP and RCMs

Also, Figure 5.5 indicates that the relative contribution to the uncertainty by HP is decreased in all simulations using BC data in comparison to the simulations using Original RCMs data. As in high flows, CF method becomes much more sensitive to HP uncertainty among SD methods and its sensitivity is even stronger than original RCMs.

5.4. Seasonality

5.4.1. High flow Analysis

In this section, the influence of SD methods on the prediction of seasonality is given. Figure 5.6 presents the predicted seasonality index by simulations using data from each data type for both periods. Figure 5.6 shows that the observed dominant high flow events occurred during autumn/winter season for the period 1961-1990 ($S_D = 0.2310$).

Simulations using BC and CF data overestimated the Seasonality index for reference period to some extent as their median values are greater than observed seasonality (Figure 5.6-a-b-c).

Some parameter files using Original RCMs' resulted in discharge outputs with minus degree seasonality index, therefore they showed some dominant high flow events for spring/summer for the period 1961-1990, as they can be seen as outliers. BC enlarges the box size and hence increasing the median of seasonality index to 0.61 for the reference period. This means that the flood events occur late in fall toward winter season with BC method. For the future period, simulations by all parameter files using Original RCM outcomes projected almost same with its reference period, yet without any outliers with minus degree seasonality index for this time. In future period, the median values of both SD methods show an index value greater than 0.5 and thus, indicating a tendency to late flood occurrence events in Fall season comparing to the reference period. The median value of original RCMs stays lower than 0.5 for future period. As in reference period the BC produces a more widespread box size in future period.

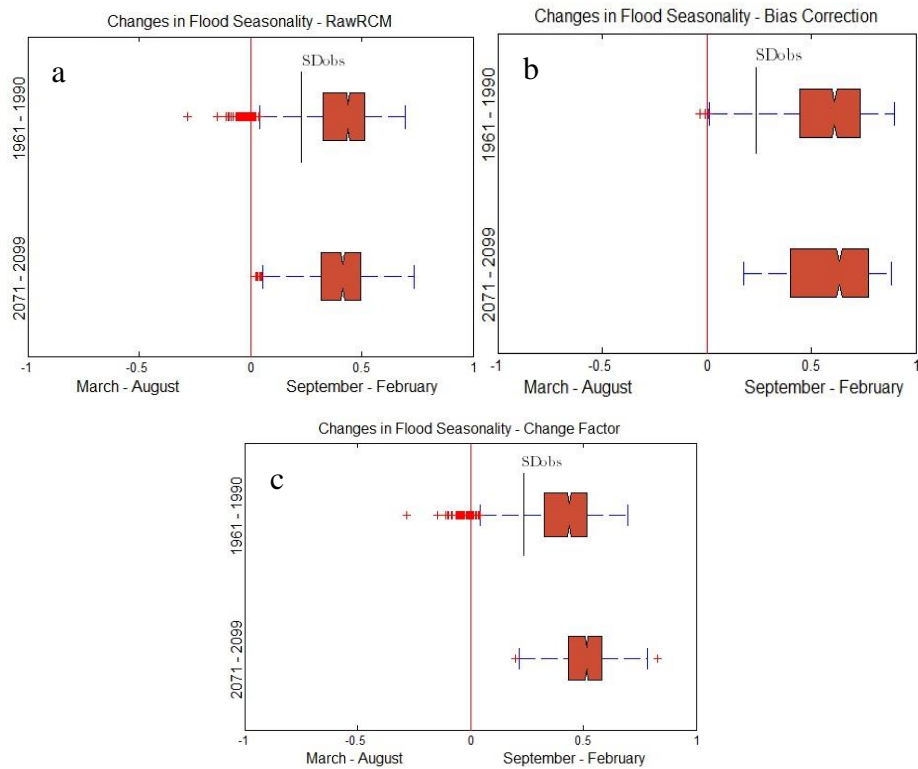


Figure 5.6. Boxplot showing seasonality index for both period for each data type, (SD_obs indicates the observed seasonality)

Model simulations using CF data projected that the dominance of extreme events in autumn/winter over spring/summer is slightly weaker than the projection by BC data for the future period.

Simulations using BC and CF data projected that the seasonality in high flow events will be greater than their reference period, which means that in the future the catchment would likely to observe more dominant high flow events in autumn/winter. The BC method that shows the most pronounced changes in flood seasonality tends to be lowest for the relative role of hydrological parameter uncertainty. This is reversed with CF method.

Because the boxes in Figure 5.6 presenting changes in flood seasonality include all RCMs and all hydrological parameterizations with all NSE functions, the partition in flood seasonality changing from each source is distinguished. Therefore, a new box plot analysis considering changes in flood seasonality from RCMs and hydrologic

parameterizations separately for each NSE function is prepared. These box plots are shown for 25 hydrological model parameter sets in Figure 5.7a and 15 RCMs in Figure 5.7b along with each NSE function for original RCM data while equivalent box plots are shown in Figure 5.8a and 5.8b for BC method and in Figure 5.9a and 5.9b for CF method.

In Figure 5.7, 5.8 and 5.9, the upper boxes in each box plot includes the averaged seasonality indexes of 25 parameter files for each of 15 RCMs, whereas the lower boxes in each box plot includes the averaged seasonality indexes of 15 RCMs for each of 25 parameter files. Therefore, upper and lower boxes represent the hydrological parameter uncertainty and climate model uncertainty in seasonality assessment to some extent, respectively.

The seasonality of floods or high flows in Omerli Basin is represented by Fall season. Especially with downscaling methods (BS and CF) the seasonality index tends to shift later times in Fall in future period. It appears that changes in flood seasonality are more pronounced in hydrological model parameterizations than that in RCM simulations for all data types (original, BC and CF). The largest change in seasonality index occurs with BC method for both reference and future period.

The results also indicated that for each data type, hydrological parameters and RCMs showed an increase in seasonality for future period relative to the reference period as mentioned before, that means that the importance of autumn/winter events is projected to increase for Omerli catchment.

Another important point to derive from the figures is that, different NSE functions used to optimize the parameter files do not seem to have much influence on seasonality prediction. Therefore, Figure 6.10 is drawn in which the simulations by parameter files from each NSE functions are combined in the single boxes, in which the same conclusions can be drawn.

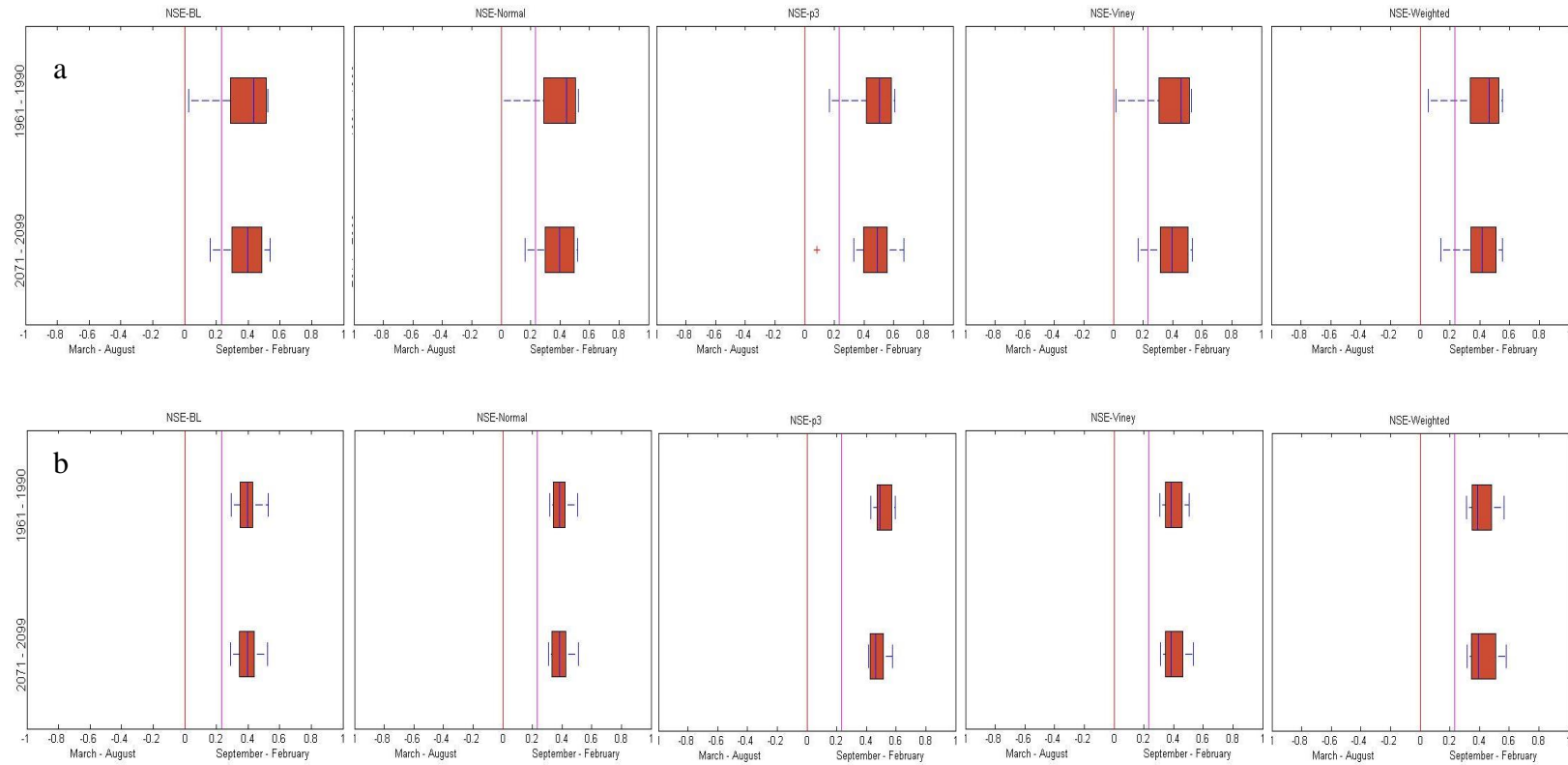


Figure 5.7 Uncertainty in seasonality due to hydrological model parameterization (a) and climate models (b) by using Original RCM data (Purple line indicates the observed seasonality from the reference period)

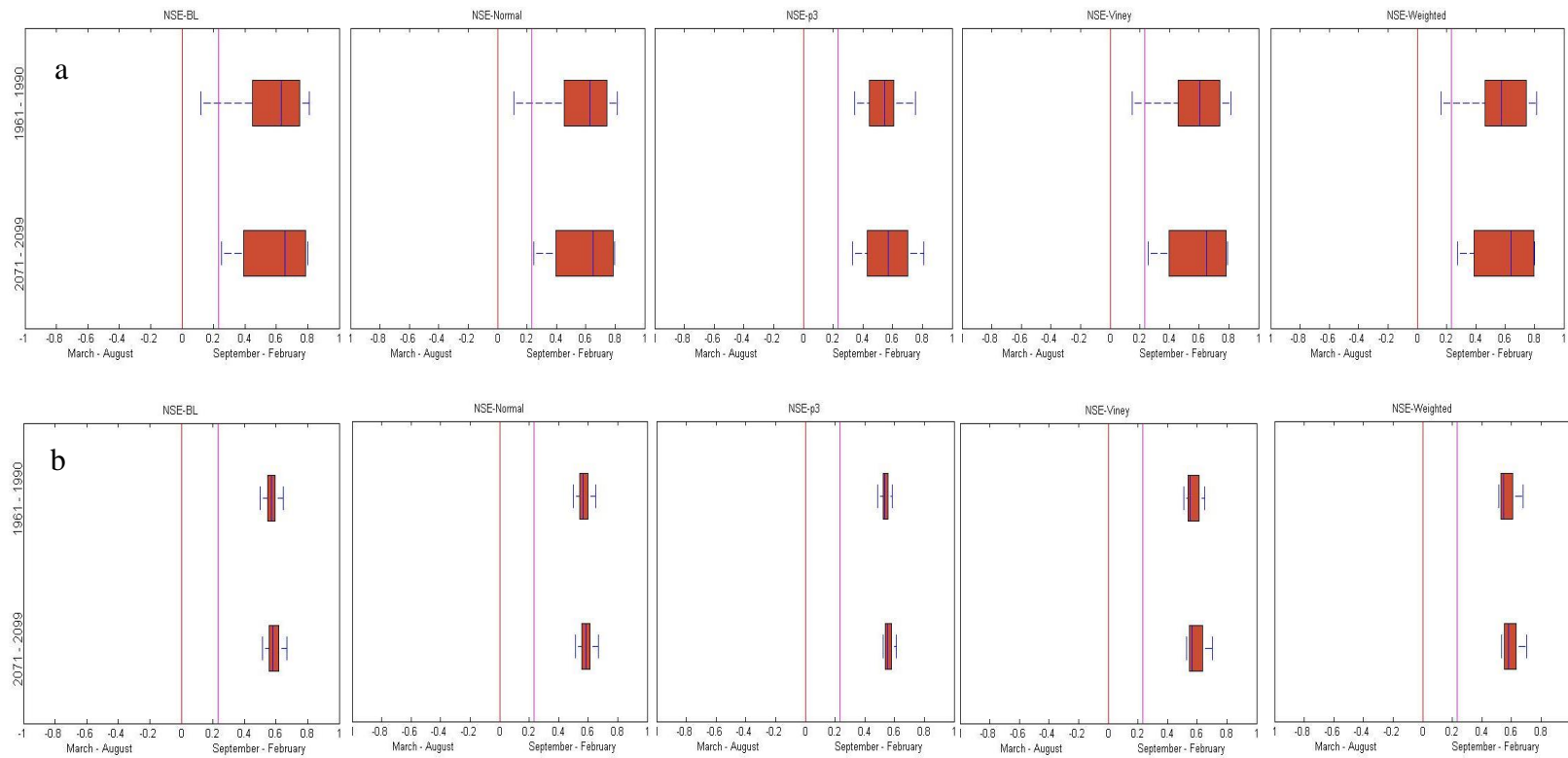


Figure 5.8 Uncertainty in seasonality due to hydrological model parameterization (a) and climate models (b) by using BC data (Purple line indicates the observed seasonality from the reference period)

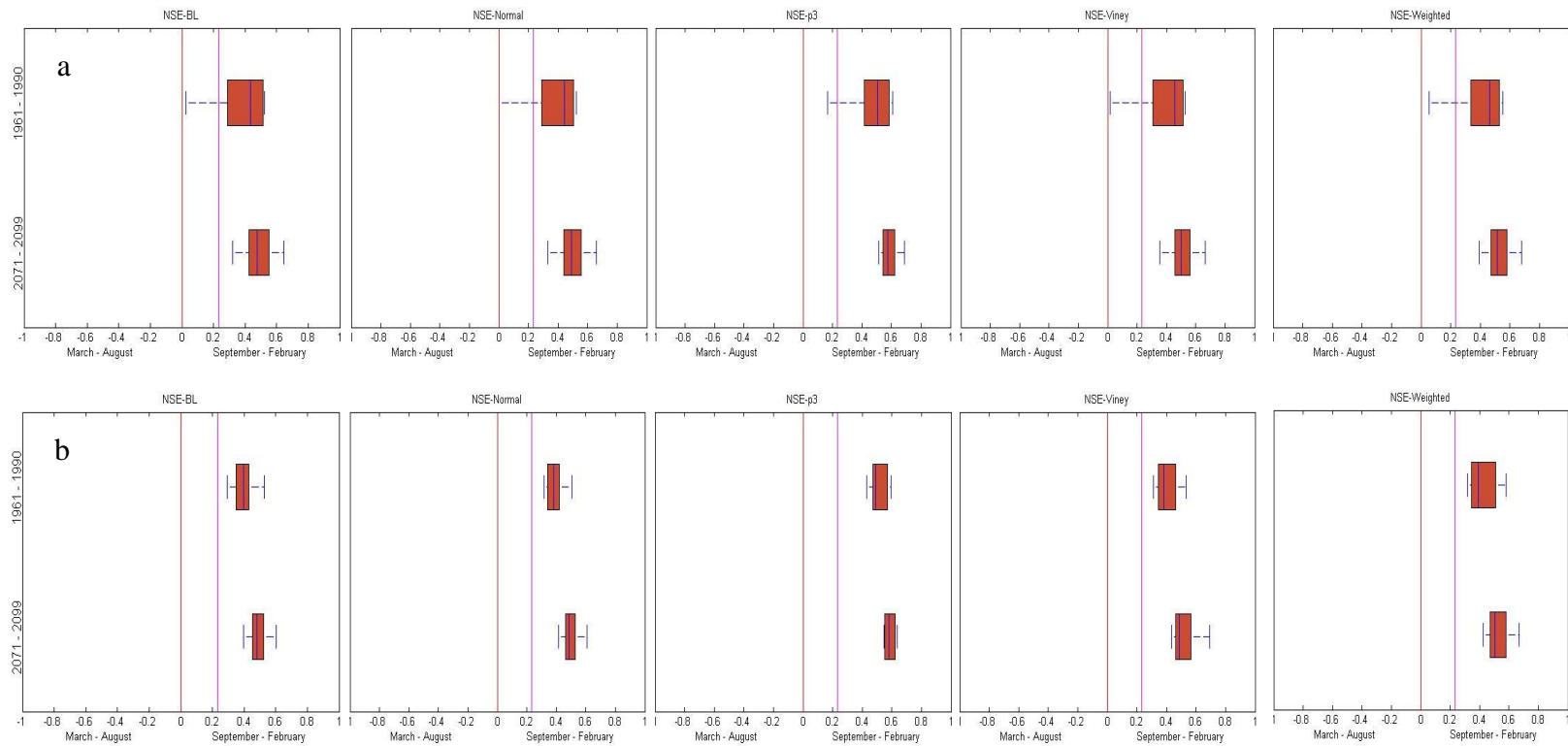


Figure 5.9 Uncertainty in seasonality due to hydrological model parameterization (a) and climate models (b) by using CF data (Purple line indicates the observed seasonality from the reference period)

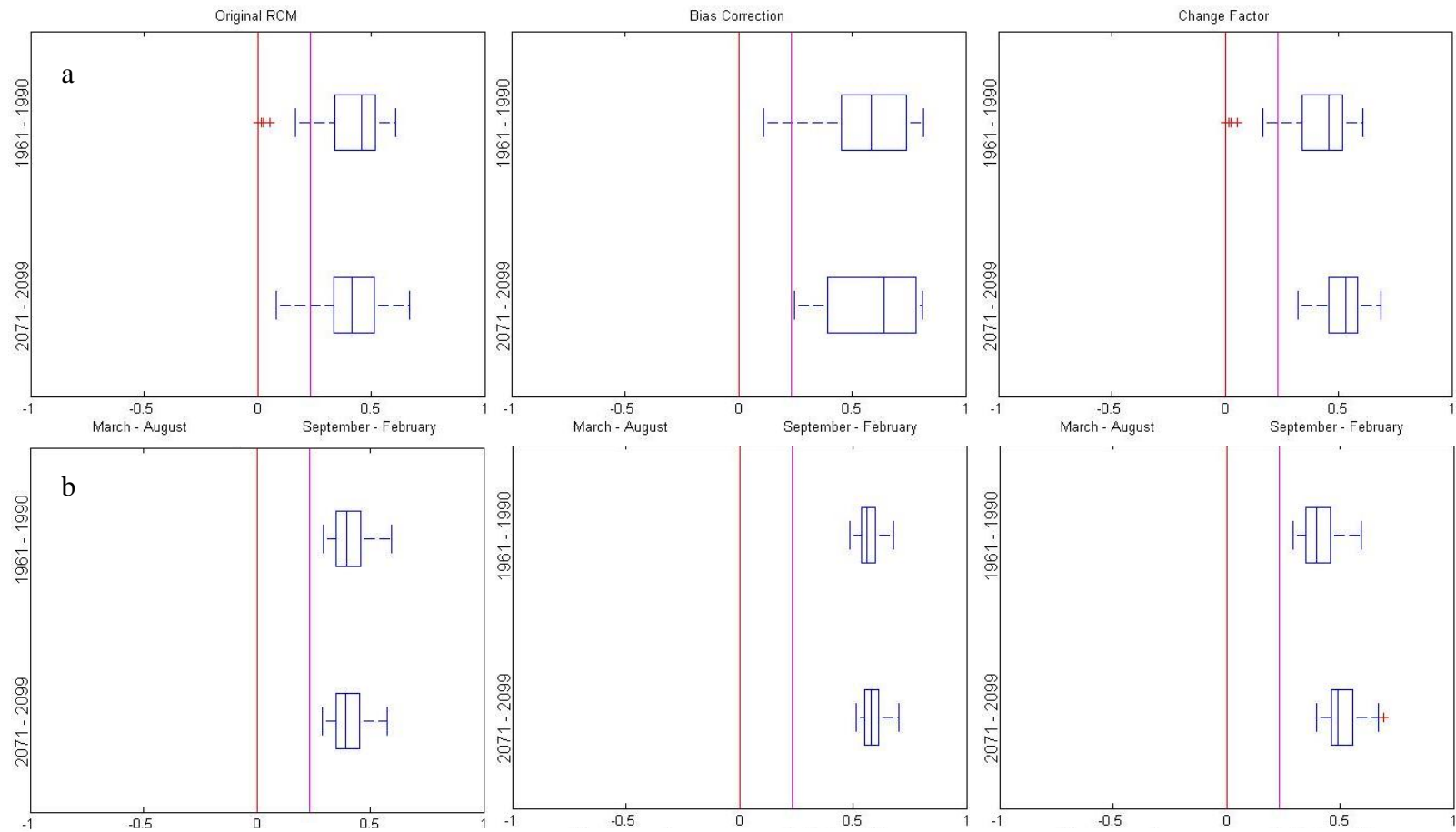


Figure 5.10 Uncertainty in seasonality due to hydrological model parameterization (a) and climate models (b) (Each box plot contains all simulations by every parameter files from each NSE function) (Purple line indicates the observed seasonality from the reference period)

CHAPTER 6

SUMMARY, CONCLUSIONS and RECOMMENDATIONS

6.1. Summary

Global warming through anthropologic forces is a proven phenomenon and its influence on hydrological components is rather complex to assess. Obscurity about future greenhouse gases emission or any other sources that would influence future climate causes great uncertainty in climate prediction. This topic is still drawing attention among the researchers, as the uncertainty arises in any studies investigating the future condition.

Many factors such as different GCM/RCM and their structure and parameterization, different emission scenario, statistical/dynamical downscaling techniques in order to make interpretation at basin scale, hydrological model structure and parameterization account most of the uncertainty in future condition (Dobler et al., 2012). In this research, it is intended to assess the uncertainty in the projected changes in high and low flow for the future period due to two factors; the parameterization of hydrological model and the temperature and precipitation inputs from different RCMs.

Daily precipitation and temperature data for the reference (1961-1990) and future (2071-2099) period obtained from the fifteen different RCM combinations with 25-km resolution based on A1B carbon emission scenario from EU-ENSEMBLES project. Observed daily precipitation and temperature records are provided by Turkish State Meteorological Service for the period 1961-2004, while daily discharges are obtained from State Hydraulic Works for the period 1978-2004. Since this study also seeks to examine the influence of different statistical downscaling on the uncertainty in the projected changes in

extreme river flows, “Bias correction in mean” and “Change Factor” SD methods are applied to RCMs’ both reference and future period. Hydrological model HBV is calibrated by using observed precipitation and temperature records for the period 1978-1985. During calibration procedure, five different objective functions (NSE_BL, NSE_Normal, NSE_p3, NSE_Viney, and NSE_Weighted) are used to optimize the HBV model, and 25 best-fit parameter files are generated for each NSE function through built-in Monte Carlo simulation. These fifteen different RCMs are used to assess the uncertainty due to the precipitation and temperature inputs, while these 25 different parameter sets for each NSE function are used to assess the uncertainty due to the hydrological parameterization.

6.2. Conclusions

The main findings of this thesis can be listed as follows:

- Regarding the reproduction of daily precipitation for the period 1961-1990 by all RCMs; predictive indicators RMSE, NSE, Correlation Coefficient R and Bias are calculated. It is observed that RCMs’ RMSE values are similar to each other, yet very fair. Regarding the NSE results, it can be inferred that the “observed mean” is a better predictor than the RCMs. There is a tendency to underestimate the precipitation by RCMs for the reference period. It is concluded that even the best RCM outputs do not seem sufficient to fully represent Omerli catchment’s daily precipitation, as their performance indicators are poor overall.
- It is demonstrated that all RCMs are able to capture the seasonality in precipitation pattern to some degree, which is wet autumn & winter and semi-dry spring & dry summer.
- The simulation results by using all parameter files for the validation period 1986-2004 demonstrated that while NSE_p3 showed worst

performance in reproducing discharge values, to some extent the others reproduced stream flow better. However, the reproduction of discharge pattern for the period 1986-2004 by the parameter files is slightly unsatisfactory.

- Regarding the discharge simulations by 25 parameter files for each NSE function for the period 1986-2004, it is noticed that there are considerable number of high flow events.
- In order to examine the influence of hydrological model parameterization on reproducing the extreme discharge for the reference period, POT analysis is carried out to obtain extreme value series for the data. The result indicated that except for NSE-p3 which overestimate the high flows, the parameter files calibrated through other NSE functions slightly underestimate the high flows compared to the observed high flows for the period 1986-2004. NSE_Weighted parameter sets seem to be the best in reproducing the high flow events for the period 1986-2004.
- Also, it is noticed that the model simulations by parameter files calibrated through each NSE function slightly overestimate the low events in comparison with the observed low flows for the period 1986-2004. As in reproducing the extreme high flow events, NSE_Weighted parameter sets seem to be the best in reproducing the extreme low events for the period 1986-2004.
- Regarding the total mean variance in the change in high-low flows from reference to future period, it is found that the statistical downscaling methods BC and CF increase the total mean variance. (Dobler et al., 2012)
- NSE_p3 outputs show substantially greater mean variances in projected changes in high-low flows among the other NSE functions.

- It is noticed that total mean variances in the projected changes in high-low flows by each NSE functions reaches its highest values in CF method. This means that CF method produces greater variance (therefore, cause more uncertainty) compared with BC.
- Regarding the relative uncertainty in projected changes in high flow events, it is found that the relative contribution to the uncertainty by climate models is greater than the uncertainty caused by hydrological model parameterization (HP) in prediction of extreme high flow events in the simulations by parameter files using each Original RCM, BC and CF data. However, both SD methods for three NSE functions (NSE_p3, NSE_Viney, NSE_Weighted) show the same trend in which NSE_p3 decreases HP fraction while NSE_Viney and NSE_Weighted increase HP fraction after the application of both SD. Overall CF becomes more sensitive to HP uncertainty.
- The results demonstrated that the relative contribution to the uncertainty by HP and RCMs differs between high flow and low flow prediction. The relative contribution to the uncertainty in projected changes in low flows by HP is increased for each NSE function in the simulations using Original RCM, BC and CF when compared to the relative uncertainty in high flow prediction.
- It is assessed that the observed dominant high flow events occurred during autumn/winter season for the period 1961-1990.
- Simulations using BC and CF data overestimated the Seasonality index for reference period to some extent as their median values are greater than both RCMs-derived observed seasonality.
- Both SD methods projected a tendency to late flood occurrence events in Fall season comparing to the reference period, which means that in the

future the catchment would likely to observe more dominant high flow events in autumn/winter. The BC method that shows the most pronounced changes in flood seasonality tends to be lowest for the relative role of hydrological parameter uncertainty. This is reversed with CF method. It appears that changes in flood seasonality are more pronounced in hydrological model parameterizations than that in RCM simulations for all data types (Original, BC and CF).

6.3. Future work recommendations

Both SD methods projected a tendency to late flood occurrence events in Fall season, which means that in the future the catchment would likely to observe more dominant high flow events in autumn/winter by the end of the 21st century in annual series under the SRES A1B emission scenario in the Omerli Basin. However, original RCMs release reversal trend in flood occurrence for the future period. Relying on fine scale information obtained through downscaling is therefore critical in hydrological assessment studies that seek water resources management. These projected seasonal changes (increase in winter and decrease in fall) in high flows should be considered in planning of Omerli dam reservoir in order to sustain the effective storage and effective use of water. Increasing in the magnitude of high flow events pose a flood risk which should be taken care of.

It is essential to mention that the calibration period should be sufficiently long so that the calibrated parameter files represent the catchment well, however; in this study due to the lack of observed discharge records the calibration period duration is only 7 years. In order to increase the reliability of the outcome of such studies on climate, it is important to have reliable observed data without any missing records.

Since CF has no unique reference period, future studies are suggested to use different statistical downscaling methods for the comparison reason.

Insufficiency of observed data is one of the biggest problem with acquiring consistent outcome when calibration of hydrological model by using observed data is carried out. Therefore, future work should pay attention to the availability of observed records. Future works could be further expanded by focusing on GCM/RCM under different emission scenarios, different hydrological model structure, and different techniques to quantify the uncertainty. Also, other source of uncertainty belonging to future variables could be studied.

REFERENCES

- Anandhi, Frei, A., Pierson, A., Schneiderman, D. C., Zion, E. M., Lounsbury, M. S., & David Matonse, A. H. (2011). Examination of change factor methodologies for climate change impact assessment. *Water Resources Research*, 47(3), W03501. doi: 10.1029/2010WR009104
- Bakanligi, T. C. v. S. (2013). Türkiye İklim Değişikliği 5. Bildirimi.
- Bergström, S. (1976). Development and application of a conceptual runoff model for Scandinavian catchments. (Ph.D.), Norrköping.
- Bergström, S. (1992). The HBV model - its structure and applications: SMHI Reports RH, No. 4, Norrköping.
- Beven, K., & Binley, A. (1992). The future of distributed models: Model calibration and uncertainty prediction. *Hydrological Processes*, 6(3), 279-298. doi: 10.1002/hyp.3360060305
- Bou-Zeid, E., & El-Fadel, M. (2002). Climate Change and Water Resources in Lebanon and the Middle East. *Journal of Water Resources Planning and Management*, 128(5), 343-355. doi: doi:10.1061/(ASCE)0733-9496(2002)128:5(343)
- Bozkurt, D., & Sen, O. L. (2013). Climate change impacts in the Euphrates–Tigris Basin based on different model and scenario simulations. *Journal of Hydrology*, 480(0), 149-161. doi: <http://dx.doi.org/10.1016/j.jhydrol.2012.12.021>
- Bozkurt, D., Turuncoglu, U., Sen, O., Onol, B., & Dalfes, H. N. (2012). Downscaled simulations of the ECHAM5, CCSM3 and HadCM3 global models for the eastern Mediterranean–Black Sea region: evaluation of the reference period. *Climate Dynamics*, 39(1-2), 207-225. doi: 10.1007/s00382-011-1187-x
- Chen, J., Brissette, F. P., Chaumont, D., & Braun, M. (2013). Performance and uncertainty evaluation of empirical downscaling methods in quantifying the climate change impacts on hydrology over two North American river basins. *Journal of Hydrology*, 479(0), 200-214. doi: <http://dx.doi.org/10.1016/j.jhydrol.2012.11.062>
- Chen, J., Brissette, F. P., & Leconte, R. (2011). Uncertainty of downscaling method in quantifying the impact of climate change on hydrology. *Journal of Hydrology*, 401(3–4), 190-202. doi: <http://dx.doi.org/10.1016/j.jhydrol.2011.02.020>

- Diaz-Nieto Jacqueline, W. R. (2005). A comparison of statistical downscaling and climate change factor methods: impacts on low flows in the River Thames, United Kingdom. *Climatic Change*, 69(2-3), 245-268. doi: 10.1007/s10584-005-1157-6
- Dobler, C., Hagemann, S., Wilby, R. L., & Stötter, J. (2012). Quantifying different sources of uncertainty in hydrological projections in an Alpine watershed. *Hydrol. Earth Syst. Sci.*, 16(11), 4343-4360. doi: 10.5194/hess-16-4343-2012
- Environment, M. o. (July 2011). Republic of Turkey National Climate Change Action Plan 2011-2023. Ankara.
- Feng, S., & Hu, Q. (2007). Changes in winter snowfall/precipitation ratio in the contiguous United States. *Journal of Geophysical Research: Atmospheres*, 112(D15), D15109. doi: 10.1029/2007JD008397
- Fischer, G., Shah, M., N. Tubiello, F., & van Velhuizen, H. (2005). Socio-economic and climate change impacts on agriculture: an integrated assessment, 1990–2080. *Philosophical Transactions of the Royal Society B: Biological Sciences*, 360(1463), 2067-2083. doi: 10.1098/rstb.2005.1744
- Frei, C., Schöll, R., Fukutome, S., Schmidli, J., & Vidale, P. L. (2006). Future change of precipitation extremes in Europe: Intercomparison of scenarios from regional climate models. *Journal of Geophysical Research: Atmospheres*, 111(D6), D06105. doi: 10.1029/2005JD005965
- Gong, Y., Shen, Z., Hong, Q., Liu, R., & Liao, Q. (2011). Parameter uncertainty analysis in watershed total phosphorus modeling using the GLUE methodology. *Agriculture, Ecosystems & Environment*, 142(3–4), 246-255. doi: <http://dx.doi.org/10.1016/j.agee.2011.05.015>
- Hartmann, D. L., A.M.G. Klein Tank, M. Rusticucci, L.V. Alexander, S. Brönnimann, Y. Charabi, F.J. Dentener, E.J. Dlugokencky, D.R. Easterling, A. Kaplan, B.J. Soden, P.W. Thorne, M. Wild and P.M. Zhai. (2013). Observations: Atmosphere and Surface In: *Climate Change 2013. Cambridge, United Kingdom and New York, NY, USA.: The Physical Science Basis. Contribution of Working Group I to the Fifth Assessment Report of the Intergovernmental Panel on Climate Change* [Stocker, T.F., D. Qin, G.-K. Plattner, M. Tignor, S.K. Allen, J. Boschung, A. Nauels, Y. Xia, V. Bex and P.M. Midgley (eds.)].
- Hidalgo, H. G., Dettinger, M. D., & Cayan, D. R. (2008). Downscaling With Constructed Analogues: Daily Precipitation And Temperature Fields Over The United States Public Interest Energy Research Program: California Energy Commission.

- Hillel, D., & Rosenzweig, C. (2012). *Handbook of Climate Change and Agroecosystems: Global and Regional Aspects and Implications* (D. Hillel Ed.): World Scientific.
- Hwang, C.-L., Lai, Y.-J., & Liu, T.-Y. (1993). A new approach for multiple objective decision making. *Computers & Operations Research*, 20(8), 889-899. doi: [http://dx.doi.org/10.1016/0305-0548\(93\)90109-V](http://dx.doi.org/10.1016/0305-0548(93)90109-V)
- Jamal Khosravi, M. A. A., Mohammad Reza Alizadeh and Mir Hosein Peyman. (2011). Application of Multiple Criteria Decision Making System Compensatory (TOPSIS) in Selecting of Rice Milling System. *World Applied Sciences Journal*, 13 (11): , 2306-2311.
- Jay Gullledge, P. D. (July 2012). *The Causes of Global Climate Change*
- Kalra, N. H., Stephane; Lempert, Robert; Brown, Casey; Fozzard, Adrian; Gill, Stuart; Shah, Ankur;. (2014). Agreeing on robust decisions : new processes for decision making under deep uncertainty *Transport Economics Policy & Planning; Climate Change Economics; Climate Change Mitigation and Green House Gases; Debt Markets; Science of Climate Change.*
- Kara, F. (2014). *Effects of Climate Change on Water Resources in Omerli Basin.* (Ph.D), Middle East Technical University, Ankara.
- Klukowska, J. (2014). *Lecture 5: Applications of Looping and Conditional Execution* (Vol. 2014).
- Knutson, T. R., McBride, J. L., Chan, J., Emanuel, K., Holland, G., Landsea, C., . . . Sugi, M. (2010). Tropical cyclones and climate change. *Nature Geosci*, 3(3), 157-163. doi: http://www.nature.com/ngeo/journal/v3/n3/supinfo/ngeo779_S1.html
- Knutti, R. (2010). The end of model democracy? *Climatic Change*, 102(3-4), 395-404. doi: 10.1007/s10584-010-9800-2
- Lawrence, D., Haddeland, I., and Langsholt, E. (2009). Calibration of HBV hydrological models using PEST parameter estimation. OSLO: Norwegian Water Resources and Energy Directorate.
- Le Treut, H., R. Somerville, U. Cubasch, Y. Ding, C. Mauritzen, A. Mokssit, T. Peterson and M. Prather. (2007). Historical Overview of Climate Change: The Physical Science Basis. Contribution of Working Group I to the Fourth Assessment Report of the Intergovernmental Panel on Climate Change [Solomon, S., D. Qin, M. Manning, Z. Chen, M. Marquis, K.B. Averyt, M. Tignor and H.L. Miller (eds.)].

- Leander, R., & Buishand, T. A. (2007). Resampling of regional climate model output for the simulation of extreme river flows. *Journal of Hydrology*, 332(3–4), 487-496. doi: <http://dx.doi.org/10.1016/j.jhydrol.2006.08.006>
- Lindenschmidt, K.-E. F., Katrin Baborowski, Martina. (2007). Structural uncertainty in a river water quality modelling system. *Ecological Modelling*, 204(3–4), 289-300. doi: <http://dx.doi.org/10.1016/j.ecolmodel.2007.01.004>
- M. Petrakis, C. G., G. Lemesios. (2014). Climate Change Models: The Cyprus Case Paper presented at the AdaptToClimate, Nicosia Cyprus.
- Maraun, D., Wetterhall, F., Ireson, A. M., Chandler, R. E., Kendon, E. J., Widmann, M., Thiele-Eich, I. (2010). Precipitation downscaling under climate change: Recent developments to bridge the gap between dynamical models and the end user. *Reviews of Geophysics*, 48(3), RG3003. doi: 10.1029/2009RG000314
- Meehl, G. A., Washington, W. M., Ammann, C. M., Arblaster, J. M., Wigley, T. M. L., & Tebaldi, C. (2004). Combinations of Natural and Anthropogenic Forcings in Twentieth-Century Climate. *Journal of Climate*, 17(19), 3721-3727. doi: 10.1175/1520-0442(2004)017<3721:CONAAF>2.0.CO;2
- Melching, C., & Yoon, C. (1996). Key Sources of Uncertainty in QUAL2E Model of Passaic River. *Journal of Water Resources Planning and Management*, 122(2), 105-113. doi: doi:10.1061/(ASCE)0733-9496(1996)122:2(105)
- Observatory, M. L. (2015, October 16, 2014). Current Carbon Dioxide level. Retrieved 26.01.2015, 2015
- OCAR, A. K., Chris Butenhoff and Martha Shearer. (2010). Climate change in Oregon: defining the problem and its causes. Oregon Climate Assessment Report.
- P. Willems, M. V. (2011). Statistical precipitation downscaling for small-scale hydrological impact investigations of climate change. *Journal of Hydrology*, 402 (2011) 193–205.
- Philippe Gachona, Y. D. (2007). Temperature change signals in northern Canada: convergence of statistical downscaling results using two driving GCMs. *International Journal of Climatology*, 27(Int. J. Climatol), 1623–1641. doi: DOI: 10.1002/joc.1582
- Prudhomme, C., Jakob, D., & Svensson, C. (2003). Uncertainty and climate change impact on the flood regime of small UK catchments. *Journal of*

Hydrology, 277(1–2), 1-23. doi: [http://dx.doi.org/10.1016/S0022-1694\(03\)00065-9](http://dx.doi.org/10.1016/S0022-1694(03)00065-9)

Prudhomme, C., Reynard, N., & Crooks, S. (2002). Downscaling of global climate models for flood frequency analysis: where are we now? *Hydrological Processes*, 16(6), 1137-1150. doi: 10.1002/hyp.1054

Reichler T, J. K. (2008). How Well Do Coupled Models Simulate Today's Climate? *Bulletin of the American Meteorological Society*, 89(3), 303-311.

Reynard, N. S., Prudhomme, C., & Crooks, S. M. (2001). The Flood Characteristics of Large U.K. Rivers: Potential Effects of Changing Climate and Land Use. *Climatic Change*, 48(2-3), 343-359. doi: 10.1023/A:1010735726818

RL. Wilby, S. C., E. Zorita, B. Timbal, P. Whetton, LO. Mearns. (2004). Guidelines for Use of Climate Scenarios Developed from Statistical Downscaling Methods Supporting material: IPCC.

Smith, T. M., Karl, T. R., & Reynolds, R. W. (2002). How Accurate Are Climate Simulations? *Science*, 296(5567), 483-484. doi: 10.1126/science.1070365

Stedinger, J. R., Vogel, R. M., Lee, S. U., & Batchelder, R. (2008). Appraisal of the generalized likelihood uncertainty estimation (GLUE) method. *Water Resources Research*, 44(12), W00B06. doi: 10.1029/2008WR006822

Sunyer, M. A., Madsen, H., & Ang, P. H. (2012). A comparison of different regional climate models and statistical downscaling methods for extreme rainfall estimation under climate change. *Atmospheric Research*, 103(0), 119-128. doi: <http://dx.doi.org/10.1016/j.atmosres.2011.06.011>

Tolson, B. A., & Shoemaker, C. A. (2007). Dynamically dimensioned search algorithm for computationally efficient watershed model calibration. *Water Resources Research*, 43(1), W01413. doi: 10.1029/2005WR004723

Van der Linden P., & Mitchell, J. F. B. (2009). ENSEMBLES: Climate Change and its Impacts: Summary of research and results from the ENSEMBLES project. Met Office Hadley Centre, FitzRoy Road, Exeter EX1 3PB, UK. 160pp.

Wilby, R. L., & Harris, I. (2006). A framework for assessing uncertainties in climate change impacts: Low-flow scenarios for the River Thames, UK. *Water Resources Research*, 42(2), W02419. doi: 10.1029/2005WR004065

- Willems, P. (2004). WETSPRO: Water Engineering Times Series PROcessing tool (Faculty of Engineering Department of Civil Engineering, Trans.): Katholieke Universiteit Leuven, Kasteelpark Arenberg 40 BE-3001 Leuven, Belgium.
- Willems, P. (2009). A time series tool to support the multi-criteria performance evaluation of rainfall-runoff models. *Environmental Modelling & Software*, 24(3), 311-321.
- Yucel, I., A. Guventurk, & Sen, O. L. (2015). Climate change impacts on snowmelt runoff for mountainous transboundary basins in eastern Turkey,. *International Journal of Climatology*,, 35, 215-228.
- Z.Y. Shen, L. Chen, & Chen, T. (2012). Analysis of parameter uncertainty in hydrological and sediment modeling using GLUE method: a case study of SWAT model applied to Three Gorges Reservoir Region, China. *Hydrol. Earth Syst. Sci.*, HESS, 16(1).
- Zahmatkesh, Z. Karamouz, M. Goharian, & E. Burian, S. (2014). Analysis of the Effects of Climate Change on Urban Storm Water Runoff Using Statistically Downscaled Precipitation Data and a Change Factor Approach. *Journal of Hydrologic Engineering*, 0(0), 05014022. doi: doi:10.1061/(ASCE)HE.1943-5584.0001064